

# NATIONAL ADVISORY COMMITTEE FOR AERONAUTICS

TECHNICAL NOTE 2294

LIFT AND PITCHING DERIVATIVES OF THIN SWEPTBACK TAPERED  
WINGS WITH STREAMWISE TIPS AND SUBSONIC LEADING  
EDGES AT SUPERSONIC SPEEDS

By Frank S. Malvestuto, Jr., and Dorothy M. Hoover

Langley Aeronautical Laboratory  
Langley Field, Va.



Washington  
February 1951

Reproduced From  
Best Available Copy

DISTRIBUTION STATEMENT A  
Approved for Public Release  
Distribution Unlimited

20000816 128

NATIONAL ADVISORY COMMITTEE FOR AERONAUTICS

TECHNICAL NOTE 2294

LIFT AND PITCHING DERIVATIVES OF THIN SWEEPBACK TAPERED  
WINGS WITH STREAMWISE TIPS AND SUBSONIC LEADING  
EDGES AT SUPERSONIC SPEEDS

By Frank S. Malvestuto, Jr., and Dorothy M. Hoover

SUMMARY

On the basis of linearized supersonic-flow theory, approximations to the static-pitching derivative  $C_{m\alpha}$ , the lift-due-to-pitching derivative  $CL_q$ , and the damping-in-pitch derivative  $C_{mq}$  were derived for a series of thin sweptback tapered wings with streamwise tips and subsonic leading edges. The effects of camber and thickness were not considered. The results are valid for a range of Mach number for which the Mach lines from the apex of the wing are ahead of the leading edge and the Mach lines from the apex of the trailing edge may traverse the wing but cannot intersect the leading edge. An additional limitation is that the inboard wing-tip Mach lines may not intersect on the wing or intersect the opposite wing tips.

The results of the analysis are given in the form of generalized equations for  $C_{m\alpha}$ ,  $CL_q$ , and  $C_{mq}$  together with a series of design curves from which rapid estimations of  $C_{m\alpha}$ ,  $CL_q$ , and  $C_{mq}$  can be made for given values of aspect ratio, taper ratio, Mach number, and leading-edge sweep. Some illustrative variations of the derivatives with these parameters are also presented. A series of design curves for the lift-curve slope  $CL_\alpha$ , which has been presented in NACA TN 1555 and NACA Rep. 970, is also included in this paper inasmuch as this quantity is needed in the transformation of the pitching derivatives from the body axes system to the stability axes system.

INTRODUCTION

The formulation of the linearized supersonic-flow theory has allowed the evaluation of stability derivatives for a variety of wing configurations at supersonic speeds. Information now exists on the theoretical stability derivatives of rectangular- and delta-wing plan

forms of zero thickness (references 1 to 7). For the sweptback tapered wing configuration with wing tips parallel to the wing plane of symmetry (hereinafter referred to as the "sweptback tapered wing"), the available stability derivatives include for a wide range of Mach number the lift-curve slope  $C_{L\alpha}$  (references 7 to 9), the damping-in-roll derivative  $C_{l_p}$  (references 8 to 10), and the lateral-force and yawing derivatives  $C_{Y_p}$  and  $C_{n_p}$ , respectively (references 11 and 12). The present paper derives the longitudinal-stability derivatives  $C_{m\alpha}$  (static-pitching moment),  $C_{Lq}$  (lift due to pitching), and  $C_{mq}$  (damping in pitch) for sweptback tapered wings at supersonic speeds. A range of supersonic speed has been considered for which the leading edge is subsonic and the trailing edge is subsonic with the additional limitations that the Mach lines from the apex of the trailing edge cannot intersect the leading edge of the wing and that the Mach lines from the leading edge of the wing tips cannot intersect on the wing or intersect the opposite wing tips.

The method of analysis adopted herein is essentially the same as the method employed in reference 8 for the evaluation of  $C_{L\alpha}$  and  $C_{l_p}$ . The results of reference 8 however are restricted by the condition that the trailing edge is supersonic. Use of the formulations of references 7 and 13 herein allows consideration to be given to the approximate effect of the subsonic trailing-edge disturbances on the pressure distribution of the influenced part of the wing that is bounded by the Mach lines from the apex of the trailing edge and the trailing edge itself (the subsonic trailing-edge region).

The results of the analysis are given in the form of generalized equations for  $C_{m\alpha}$ ,  $C_{Lq}$ , and  $C_{mq}$  together with a series of design curves from which rapid estimations of  $C_{m\alpha}$ ,  $C_{Lq}$ , and  $C_{mq}$  can be made for given values of aspect ratio, taper ratio, Mach number, and leading-edge sweep. Some illustrative variations of the derivatives with these parameters are also presented. A series of design charts for the lift-curve slope  $C_{L\alpha}$ , which has been given in references 7 and 8, is also included in this paper inasmuch as this quantity is needed in the transformation of the pitching derivatives from the body axes system to the stability axes system.

#### SYMBOLS

$x, y, z$	Cartesian coordinates of an arbitrary point
$X, Y, Z$	forces parallel to $x$ , $y$ , and $z$ body axes or stability axes, respectively

$\xi, \eta$	x-coordinate and y-coordinate of a point source in xy-plane
$u_i, v_i, w_i$	induced flow velocities along x, y, and z body axes
$u', v', w'$	incremental flight velocities along x, y, and z stability axes
$u, v$	oblique coordinates in plane of wing, the axes of which are parallel to Mach lines $\left(u = \frac{M}{2B}(\xi - B\eta) \text{ and } v = \frac{M}{2B}(\xi + B\eta)\right)$
$u_w, v_w$	oblique coordinates of a particular point on surface of wing
$V$	flight speed
$\alpha$	angle of attack $(w'/V)$
$q$	angular velocity about y body axis; pitching velocity
$M$	stream Mach number $(V/\text{Speed of sound})$
$S$	wing area
$\mu$	Mach angle
$B$	cotangent of Mach angle $\left(\sqrt{M^2 - 1}\right)$
$\epsilon$	angle between leading edge and axis of wing symmetry
$\Lambda$	leading-edge sweep $(90^\circ - \epsilon)$
$\theta_o = \tan \epsilon$	
$\delta$	angle between trailing edge and axis of symmetry
$m = \frac{\tan \epsilon}{\tan \mu} = \theta_o B$	
$n = \frac{\tan \epsilon}{\tan \delta} = 1 - (1 - \lambda)\omega$	
$v = \frac{y}{x\theta_o}$	
$b$	wing span
$c_r$	wing root chord

- $c_t$  wing tip chord
- $\bar{x}$  arbitrary distance along x-axis from apex of wing
- $\lambda$  taper ratio ( $c_t/c_r$ )
- $A$  aspect ratio  $\left(\frac{b^2}{S} = \frac{2b}{(1+\lambda)c_r}\right)$
- $\omega$  geometric parameter of wing  $\left(\frac{2\theta_0 c_r}{b} = \frac{4\theta_0}{A(1+\lambda)} = \frac{4m}{AB(1+\lambda)}\right)$
- $S_W$  region of wing
- $\phi$  perturbation velocity potential on upper surface of wing
- $P$  local pressure difference between lower and upper surface of airfoil; positive in sense of lift
- $\rho$  density of air
- $C_p$  pressure coefficient  $\left(P/\frac{1}{2}\rho V^2\right)$
- $\bar{c}$  mean aerodynamic chord  

$$\left(\frac{2}{S} \int_0^{b/2} (\text{Local chord})^2 dy = \frac{2c_r [3\omega^2 - 3\omega(1-n) + (1-n)^2]}{3\omega^2(1+\lambda)}\right)$$
- $g$  B times cotangent of trailing-edge sweep angle measured from y-axis ( $B \cot \delta$ )
- $k = \sqrt{1 - g^2}$
- $K'(g)$  complete elliptic integral of first kind with modulus  $k$   

$$\left(\int_0^{\pi/2} \frac{dz}{\sqrt{1 - k^2 \sin^2 z}}\right)$$
- $E'(g)$  complete elliptic integral of second kind with modulus  $k$   

$$\left(\int_0^{\pi/2} \sqrt{1 - k^2 \sin^2 z} dz\right)$$
- $E'(m) = E\left(\sqrt{1 - m^2}\right)$
- $K'(m) = K\left(\sqrt{1 - m^2}\right)$

$M'$  pitching moment

$L$  normal force (approx. lift)

$C_L$  lift coefficient  $\left( L / \frac{1}{2} \rho V^2 S \right)$

$C_m$  pitching-moment coefficient  $\left( M' / \frac{1}{2} \rho V^2 S \bar{c} \right)$

$C_X$  longitudinal-force coefficient

$$C_{m_\alpha} = \left( \frac{\partial C_m}{\partial \alpha} \right)_{\alpha \rightarrow 0}$$

$$C_{L_q} = \left[ \frac{\partial C_L}{\partial (q \bar{c} / 2V)} \right]_{q \rightarrow 0}$$

$$C_{m_q} = \left[ \frac{\partial C_m}{\partial (q \bar{c} / 2V)} \right]_{q \rightarrow 0}$$

$$C_{m_u} = \left[ \frac{\partial C_m}{\partial (u/V)} \right]_{u \rightarrow 0}$$

$$C_{X_q} = \left[ \frac{\partial C_X}{\partial (q \bar{c} / 2V)} \right]_{q \rightarrow 0}$$

Subscripts:

ex, in region of wing external to wing-tip Mach cone and within wing-tip Mach cone, respectively

$( )_\alpha, ( )_q$  when associated with  $\phi$ ,  $P$ , and  $C_p$  indicate velocity potential, pressure, and pressure coefficient for angle of attack and pitching, respectively

## ANALYSIS

### Scope

The types of wings considered in this paper are sketched in figure 1. In the following analysis and in the figures the wing plan form with sweptback trailing edge (fig. 1(a)) is generally considered and sketched

as the typical wing, but the results are equally valid for the wing plan form with the sweptforward trailing edge (fig. 1(b)). The orientation of the wing with respect to a body system of coordinate axes used in the analysis is indicated in figure 2(a). The surface velocity potentials, the basic pressure distribution, and the stability derivatives are derived with respect to this system. Figure 2(b) shows the wing oriented with respect to the stability axes system with the origin of the system at the arbitrary point  $(\bar{x}, 0, 0)$  rearward of the apex of the wing. The transformation formulas that allow the determination of the derivatives with respect to the stability system once they are known with respect to the body axes system are presented in table 1.

The analysis is limited to wings of vanishingly small thickness that have zero camber and are not yawed with respect to the stream direction. The derivatives are valid for a range of Mach number for which the leading edge is subsonic and the trailing edge is either supersonic or subsonic with limitations. The limitation on the trailing edge when subsonic is that the Mach lines emanating from the trailing edge of the root chord cannot intersect the leading edges of the wing. An additional restriction adhered to in this paper is that the Mach lines progressing from the leading edges of the wing tips cannot intersect on the wing or intersect the opposite wing tip.

### Basic Considerations

The evaluation of the derivatives  $C_{m\alpha}$ ,  $C_{Lq}$ , and  $C_{mq}$  essentially involves a knowledge of the lifting-pressure distribution over the wing associated with angle of attack for  $C_{m\alpha}$  and with pitching for  $C_{Lq}$  and  $C_{mq}$ . These lifting-pressure coefficients can be determined from the well-known relationships

$$\left. \begin{aligned} C_P &= \frac{2\rho V u_i}{\frac{1}{2}\rho V^2} \\ \text{or} \\ C_P &= \frac{4}{V} \frac{\partial}{\partial x} \phi(x, y) \end{aligned} \right\} \quad (1)$$

where  $\phi(x, y)$  is the velocity potential on the upper surface of the wing under consideration. The potential  $\phi(x, y)$  can be determined by a particular distribution of surface sources or doublets which allows the velocity potential to satisfy the linearized partial-differential equation of the flow and the boundary conditions that are associated with the wing in its prescribed motion.

The methods presented in the analysis of reference 8 are used herein to evaluate the pressure distributions. The wing is imagined as basically consisting of two parts: the segment of the wing external to the Mach cones springing from the leading edges of the wing tips and the segment of the wing within the wing-tip Mach cones (the wing-tip region). The pressure distribution for the wing region external to the wing-tip Mach cones is precisely the same as the pressure distribution for the corresponding section of the delta wing for the same value of Mach number and leading- and trailing-edge sweep. For angle of attack and pitching, the associated pressure distributions for the part of the wing external to the wing-tip cones, when the effect of the subsonic trailing-edge disturbance is neglected, have been evaluated in references 4 and 5, respectively.

The effect of the subsonic trailing edge in producing changes in the flow in the subsonic trailing-edge region relative to the flow that would exist if the subsonic trailing-edge disturbances were disregarded (basic flow) has been analyzed in reference 7 for angle of attack and in reference 13 for pitching. The results of these two references indicate a reduction of pressure in the trailing-edge region that is necessary in order to satisfy the condition of zero pressure along the trailing edge when subsonic. These reductions in pressure and the corresponding reductions in the lift and moments were theoretically expressed in terms of corrections to these same quantities associated with the basic flow. The part of the entire subsonic-edge correction called the "symmetrical-wake correction" in reference 7 and considered in reference 13 only for pitching contains practically the entire effect of the total correction for the wings considered herein. These approximate corrections, therefore, were used and were obtained directly as subsonic trailing-edge corrections to the derivative  $C_{m_\alpha}$  from reference 7 and to the derivatives  $C_{L_q}$  and  $C_{m_q}$  from reference 13.

The pressure distribution within the wing-tip Mach cone remains to be determined. The results of the analysis of reference 8 based upon the point-source method of Evvard (reference 14) provides a sound approximation to the surface velocity potential for this region. If the notation of reference 8 is used, the potential may be expressed as (fig. 3(a))

$$\phi(x,y) = \frac{V}{\pi} \iint_{S_{W,0}} \frac{\alpha(\xi,\eta) d\xi d\eta}{\sqrt{(x-\xi)^2 - B^2(y-\eta)^2}} \quad (2)$$



where  $\alpha(\xi, \eta)$  would be merely a constant for the angle-of-attack case and would equal  $q\xi/V$  for the pitching about the apex of the wing. Differentiation of the potential given by equation (2) with respect to  $x$  gives essentially the pressure distribution in the wing-tip region for the supersonic trailing edge. For cases where the trailing edge is subsonic, the subsonic-edge corrections mentioned previously need to be considered.

### Derivative $C_{m_\alpha}$

The derivative  $C_{m_\alpha}$  for the entire wing may be expressed as

$$C_{m_\alpha} = (C_{m_\alpha})_{\text{ex}} + (C_{m_\alpha})_{\text{in}} + \Delta C_{m_\alpha}$$

The term  $\Delta C_{m_\alpha}$  is the approximate subsonic trailing-edge correction to the derivative  $C_{m_\alpha}$ . This correction has been evaluated in reference 7. The derivative  $C_{m_\alpha}$  referred to the apex of the wing may also be expressed as

$$C_{m_\alpha} = -\frac{1}{\alpha S \bar{c}} \iint_S x (C_P)_\alpha \, dx \, dy + \Delta C_{m_\alpha}$$

where  $(C_P)_\alpha$  the lifting-pressure coefficient for a wing at constant angle of attack  $\alpha$  is the sum  $(C_{P_{\text{ex}}})_\alpha + (C_{P_{\text{in}}})_\alpha$  of the lifting pressures in regions of the wing external and internal to the wing-tip Mach cones. The derivative  $C_{m_\alpha}$  may now be expressed as (fig. 3(b))

$$\begin{aligned} C_{m_\alpha} &= -\frac{1}{\alpha S \bar{c}} \iint_S x \left[ (C_{P_{\text{ex}}})_\alpha + (C_{P_{\text{in}}})_\alpha \right] dx \, dy + \Delta C_{m_\alpha} \\ &= -\frac{2}{\alpha S \bar{c}} \left[ \iint_{\substack{\text{Region} \\ \text{Ohg} + \text{Oge}}} x (C_{P_{\text{ex}}})_\alpha \, dx \, dy \right] - \\ &\quad \frac{2}{\alpha S \bar{c}} \left[ \iint_{\substack{\text{Region} \\ \text{egf}}} x (C_{P_{\text{in}}})_\alpha \, dx \, dy \right] + \Delta C_{m_\alpha} \end{aligned} \quad (3)$$

The nondimensional lifting pressure  $(C_{P_{\text{ex}}})_\alpha$  is the conical pressure for the triangular wing for the same ratio of leading-edge sweep to Mach

line sweep as the wings considered herein. From reference 4 its value in terms of the conical coordinate  $v$  is given by

$$(C_{Pex})_{\alpha} = \frac{4\theta_0\alpha}{E'(m)\sqrt{1-v^2}} \quad (4)$$

where  $E'(m)$  is the complete elliptic integral of the second kind with modulus  $\sqrt{1-m^2}$  and is plotted in figure 4. The lifting-pressure coefficient in the wing-tip region is given approximately by

$$(C_{Pin})_{\alpha} = \frac{8\alpha\theta_0\sqrt{b-2y}}{\pi\sqrt{2(1+m)(\theta_0x+y)}} \quad (5)$$

The variables  $x$  and  $y$  are restricted to variations within the wing-tip region. The expression for  $(C_{Pin})_{\alpha}$  was evaluated in reference 8 by use of the approximate potential for this region defined by equation (2). Substitution of the lifting-pressure components of the wing given by equations (4) and (5) into equation (3) and a consideration of the limits of integration (refer to fig. 3(b)) allows the derivative  $C_{m_{\alpha}}$  to be expressed in the following integral form:

$$\begin{aligned} C_{m_{\alpha}} = & -\frac{8c_r 3\theta_0^2}{3E'(m)S\bar{c}} \int_0^{\frac{1-\omega+m}{(1+m)n+m\omega}} \frac{dv}{(1-nv)^3\sqrt{1-v^2}} - \\ & \frac{(1+m)^3 b^3}{3\theta_0 E'(m)S\bar{c}} \int_{\frac{1-\omega+m}{(1+m)n+m\omega}}^1 \frac{dv}{(1+nv)^3\sqrt{1-v^2}} - \\ & \frac{16\theta_0}{\pi S\bar{c}} \int_{\frac{1+m-\omega}{n+m} \frac{b}{2}}^{b/2} \int_{\frac{1+m}{\theta_0} \frac{b}{2} - By}^{c_r + \frac{yn}{\theta_0}} \frac{x\sqrt{b-2y} \, dx \, dy}{\sqrt{2(1+m)(\theta_0x+y)}} + \\ & \frac{2m^2}{BgE'(m) \left[ 3\omega^2 - 3\omega(1-n) + (1-n)^2 \right]} \left\{ n \left[ 1 - \frac{E'(g)}{K'(g)} \right] + 3\omega \left[ 1 - \frac{\pi}{2K'(g)} \right] \right\} \end{aligned} \quad (6)$$

The complete elliptic integrals of the second kind,  $E'(m)$  and  $E'(g)$ , and the complete elliptic integral of the first kind,  $K'(g)$ , are presented

in figure 4. In equation (6) for  $C_{m\alpha}$ , the first two integrals represent the contribution of the wing region external to the wing-tip Mach cones. The third integral is the contribution of the wing-tip region and the last term is the subsonic trailing-edge correction as obtained from reference 7. Because of the conical nature of the pressure fields for the region of the wing external to the wing-tip Mach cones, the first two integrals of equation (6) are expressed in terms of the conical coordinate  $v$  which is proportional to the slope of a ray from the apex of the wing. The result of carrying out the integrations in equation (6) yields the following simplified expression for  $C_{m\alpha}$  of the entire wing in terms of  $m$ ,  $n$ ,  $A$ , and  $\omega$ :

$$C_{m\alpha} = \frac{2m}{\pi[3\omega^2 - 3\omega(1-n) + (1-n)^2]} \left[ \frac{1}{E'(m)} \left( \frac{\omega(m-1)^2[3mn - \omega m(\omega^2 - b) - n(\omega^2 - 1)(1+m)] + m(\omega^2 - 1)^2[4n + 3m - mn^2 + m\omega(1-m)]}{(n^2 - 1)^2(m-1)^2(n+m)^2} \right) \left[ \frac{(1+m)(1+n) + \omega(m-1)}{(1+m)(1+n) + \omega(m-1)} \right] (\omega+n-1)(1+m) + \right. \\ \left. \frac{\omega^3(n^2 + 2)}{(n^2 - 1)^2 \sqrt{1-n^2}} \left[ \frac{\sin^{-1} \frac{(1+m)(\omega^2 - 1) + \omega(m+1)}{\omega(m+n)}}{\omega(m+n)} - \sin^{-1} \frac{1}{\omega(m+n)} \right] + \frac{\omega^3(n^3 - kn)}{(n^2 - 1)^2} - \frac{\sqrt{1-n^2}(\omega^2 + 2)}{(1-m)^{3/2}} \left[ \frac{\sin^{-1} \frac{\omega(1-m) - mn - 1}{n+m}}{n+m} + \frac{\pi}{2} \right] + 3m \left[ \frac{1 - \frac{E'(g)}{K'(g)}}{K'(g)} + 3m \left[ \frac{1 - \frac{E'(g)}{K'(g)}}{K'(g)} \right] \right] \right) + \\ \left. \frac{8}{\pi \sqrt{1+m}} \left( \frac{-(1+m)(1+n) + \omega(m-1)}{(n+m)^2(1-m)(1+n)} \right)^{3/2} - \frac{(1+n-\omega)(2-n) - 2m(1+n)}{1+n} \left\{ \frac{(n+\omega)(n-m) - (n+m) + 2(\omega-1)}{-8(1+n)(n+m)^2} \left[ \frac{(1+m)(1+n) + \omega(m-1)}{(1+m)(1+n) + \omega(m-1)} \right] (\omega+n-1) - \right. \right. \\ \left. \left. \frac{(1+n+\omega)^2}{16(1+n)^{3/2}} \left[ \frac{\sin^{-1} \frac{(n+\omega)(n-m) - (n+m) + 2(\omega-1)}{(1+n+\omega)(n+m)}}{(1+n+\omega)(n+m)} + \frac{\pi}{2} \right] - \frac{2m+1}{1-m} \left[ \frac{(\omega-1) - m(\omega+n)}{-2(1-m)(n+m)^2} \sqrt{(1+m)(1+n) + \omega(m-1)} \right] (\omega+n-1) - \frac{1}{2(1-m)^{3/2}} \left[ \frac{\sin^{-1} \frac{(\omega-1) - m(\omega+n)}{n+m}}{n+m} + \frac{\pi}{2} \right] \right\} \right) \quad (7a)$$

$$C_{m\alpha} = \frac{8}{\pi[3\omega^2 - 3\omega(1-n) + (1-n)^2]} \left( \frac{-15mn[2n(1-n) - \omega(4-n)] - 2(n-1)^2[7(2n+\omega)^2 + 4(2-\omega)(3n+\omega+1)]}{15(n-1)^2(1+n)^{5/2}} \sqrt{\omega+n-1} + \frac{\omega^3(\omega^2 + 2)}{2(n^2 - 1)^2 \sqrt{1-n^2}} \left[ \frac{\sin^{-1} \frac{2(n-1) + \omega}{\omega}}{\omega} - \sin^{-1} \frac{1}{\omega} \right] + \right. \\ \left. \frac{\omega^3(n^3 - kn)}{2(n^2 - 1)^2} - 2 \left[ \frac{(4+n-9m)\sqrt{2(\omega-1+n)}}{30(1+n)^{5/2}} - \frac{2(2m-1) - n(1-n-\omega)}{2(1+n)} \left[ \frac{(n+\omega-3)\sqrt{2(\omega-1+n)}}{-8(1+n)^{3/2}} - \frac{(1+n+\omega)^2}{16(1+n)^2} \left( \frac{\sin^{-1} \frac{\omega+n-3}{1+n+\omega} + \frac{\pi}{2} \right) \right] \right] \right) \quad (7b)$$

For  $m = 1$ , the Mach lines from the wing apex coincide with the leading edges of wing and equation (7a) becomes

Derivative  $C_{Lq}$ 

The derivative  $C_{Lq}$  is evaluated in a manner similar to that used for  $C_{m\alpha}$ . Inasmuch as the lifting pressure due to pitching in the wing-tip region is not available, an expression for this lifting pressure in the wing-tip region must be derived. Initially however, consideration is given to the lifting pressure and the corresponding lift for the part of the wing external to the wing-tip Mach cones.

Region of wing external to wing-tip Mach cones.- For the region of the wing external to the wing-tip Mach cones, the pressure coefficient is obtained from reference 5 as

$$(C_{P_{ex}})_q = \frac{4q\theta_0 G(m)}{V} \left[ \frac{x(2 - v^2)}{\sqrt{1 - v^2}} \right] \quad (8)$$

where  $G(m)$  is an elliptic integral factor and is plotted in figure 4. The corresponding lift coefficient (origin at apex of wing) is given by

$$\begin{aligned} (C_{Lq})_{ex} &= \frac{\partial (C_L)_{ex}}{\partial (q\bar{c}/2V)} = \frac{2V}{q\bar{S}\bar{c}} (L)_q \\ &= \frac{4V}{q\bar{S}\bar{c}} \left[ \int_{\text{Region Ohg}} (C_{P_{ex}})_q dv + \int_{\text{Region Oge}} (C_{P_{ex}})_q dv \right] \\ &= \frac{16\theta_0^2 c_r^3 G(m)}{3\bar{S}\bar{c}} \int_0^{\frac{1-\omega+m}{(1+m)n+m\omega}} \frac{(2 - v^2)dv}{(1 - nv)^3 \sqrt{1 - v^2}} + \\ &\quad \frac{2b^3(1 + m)^3 G(m)}{3\theta_0 \bar{S}\bar{c}} \int_{\frac{1-\omega+m}{(1+m)n+m\omega}}^1 \frac{(2 - v^2)dv}{(1 + mv)^3 \sqrt{1 - v^2}} \quad (9) \end{aligned}$$

Region of wing within wing-tip Mach cones.- For the region of the wing within the wing-tip Mach cones, the lift due to pitching is evaluated by use of the approximate surface velocity potential expressed by equation (2); that is,

$$\phi(x, y) = \frac{V}{\pi} \iint_{S_{W,0}} \frac{\alpha(\xi, \eta) d\xi d\eta}{\sqrt{(x - \xi)^2 - B^2(y - \eta)^2}}$$

The velocity potential given by equation (2) can be modified, as stated previously, to apply to the pitching wing by consideration of the local downwash of the airfoil surface. For the thin wings of zero camber considered herein, the local angle of attack along any line, defined by  $x$  equals a constant, is equal to  $q\xi/V$  where  $q\xi$  is the local downwash. Substitution of  $q\xi/V$  for  $\alpha$  into equation (2) gives the following approximate linearized surface velocity potential for the region of the pitching wing within the wing-tip Mach cones (axes at apex of wing):

$$(\phi)_q = \frac{q}{\pi} \iint_{S_{W,0}} \frac{\xi d\xi d\eta}{\sqrt{(x - \xi)^2 - B^2(y - \eta)^2}} \quad (10)$$

The evaluation of the integral of equation (10) is carried out in the appendix. The following expression for the potential is obtained:

$$(\phi)_q = \frac{q}{3\pi B(1+m)^{3/2}} \left\{ \left[ 2(3+2m)x + 2mBy - bB(1+m) \right] \sqrt{2B(mx + By)(b-2y)} \right\} \quad (11)$$

Differentiation of the potential given in equation (11) yields the following pressure distribution for the wing-tip region:

$$\begin{aligned} (C_{P_{in}})_q &= \frac{4}{V} \frac{\partial}{\partial x} (\phi)_q \\ &= \frac{4q}{3\pi V} \left\{ \frac{6\theta_0(3+2m)x + (12+8m+2m^2)y - bm(1+m)}{(1+m)^2} \right. \\ &\quad \left. \sqrt{\frac{(1+m)(b-2y)}{2(\theta_0 x + y)}} \right\} \quad (12) \end{aligned}$$

It should be noted that, for equations (11) and (12), the variables  $x$  and  $y$  are restricted to the part of the wing within the wing-tip Mach cone. The nondimensional lift due to pitching for

the region of the wing within the wing-tip Mach cones may now be expressed as follows (for limits of integration, see fig. 3(b)):

$$C_{Lq} = \frac{16}{3\pi Sc} \int_{\frac{1+m-\omega}{n+m} \frac{b}{2}}^{b/2} \int_{\frac{1+m}{\theta_0} \frac{b}{2} - By}^{c_r + \frac{n}{\theta_0} y} \left[ \frac{6\theta_0(3+2m)x + (12+8m+2m^2)y - bm(1+m)}{(1+m)^2} \right] \sqrt{\frac{(1+m)(b-2y)}{2(\theta_0 x + y)}} dx dy \quad (13)$$

The subsonic trailing-edge correction remains to be evaluated. An excellent approximation to the complete subsonic trailing-edge correction is derived in reference 13 and may be expressed as

$$\Delta C_{Lq} = - \frac{8m^2 G(m)}{g \left[ 3\omega^2 - 3\omega(1-n) + (1-n)^2 \right]} \left\{ \left[ 1 - \frac{\pi}{2} \frac{1}{K'(g)} \right] + n \left[ 1 - \frac{E'(g) - g^2 K'(g)}{K'(g) - E'(g)} \right] \right\} \quad (14)$$

The elliptic integral  $K'(g)$  is plotted as a function of  $g$  in figure 4.

The sum of expressions (9), (13), and (14) is the lift-due-to-pitching coefficient for the entire wing. Evaluation of the integrals in these formulas gives the following expression for  $C_{Lq}$  for the axis of rotation located at the apex of the wing:

$$C_{Lq} = \frac{\omega^2}{2\sqrt{3\omega^2 - 3\omega(1-n) + (1-n)^2}} \left[ \frac{3\omega(m)}{\omega(2n^2 - 1)(n^2 - 1)(1+m) + \omega[2n^2(1-nm) + (5nm+1)]} \sqrt{\frac{[(1+m)(1+n) + \omega(m-1)](\omega+n-1)(1+m) - \omega^3(2n^3 - 5n)}{3(n^2 - 1)^2}} \right]$$

$$\frac{\omega^2}{(n^2 - 1)^2} \left[ \frac{\sin^{-1} \frac{(n^2 - 1)(1+m) + \omega(1+nm)}{\omega(n+n)}}{\sqrt{1-n^2}} - \sin^{-1} n \right] + \frac{\sqrt{1+n}}{(1-n)^{3/2}} \left[ \frac{\sin^{-1} \frac{\omega(1-m) - nm - 1}{n+m}}{\sqrt{1-n^2}} - \frac{1}{2} \right] -$$

$$\left[ \frac{(-2m^2 + 5nm + 2n^2 + 1) - \omega(2m^2 - 1)(m-1)}{3(m-1)^2(n+m)^2} \sqrt{\frac{[(1+m)(1+n) + \omega(m-1)](\omega+n-1)(1+m) - \frac{2m}{3\omega} \left[ 1 - \frac{\pi}{2K'(g)} \right] + n \left[ 1 - \frac{\pi}{K'(g)} - \frac{E^2 K'(g)}{K'(g)} \right]}{2}} \right] +$$

$$\frac{8}{\pi(1+m)^{3/2}} \frac{(n+m)(3-m)(1+m)}{3(1+n)(1-m)(n+m)} \left\{ \frac{(1+m)(1+n) + \omega(m-1)}{(1-m)^2} \right\}^{3/2} + \frac{(3+m)}{(1-m)^2} \left\{ \frac{(\omega-1) - m(\omega+n)}{-2(n+m)^2} \right\} \sqrt{\frac{[(1+m)(1+n) + \omega(m-1)](\omega+n-1)}{(1-m)^2}} -$$

$$\frac{1}{2\sqrt{1-m}} \left[ \frac{\sin^{-1} \frac{(\omega-1) - m(\omega+n)}{n+m}}{\sqrt{1-n^2}} + \frac{\pi}{2} \right] - \frac{(1+n-\omega)(3m+2nm+m^2) + 2(1+n)[\omega(3+2m) - m(1+m)]}{(1+n)^2} \left\{ \frac{(n+\omega)(n-m) - (n+m)}{-8(n+m)^2} \right\} \sqrt{\frac{[(1+m)(1+n) + \omega(m-1)](\omega+n-1)}{(1-m)^2}} -$$

$$\frac{(1+n+\omega)^2}{16\sqrt{1+n}} \left[ \frac{\sin^{-1} \frac{(n+\omega)(n-m) - (n+m)}{(1+n+\omega)(n+m)}}{\sqrt{1-n^2}} - \frac{(n+m)}{K'(n)} \right] \left( \frac{1}{2} + \frac{1}{K'(n)} \right) \quad (15a)$$

For  $n = 1$ , the Mach lines from the wing apex coincide with the leading edges of the wing and equation (15a) becomes

$$C_{Lq} = \frac{1}{\pi B(1+n)^2} \frac{32}{3\omega^2 - 3\omega(1-n) + (1-n)^2} \left[ \frac{1}{3(n-1)} \left\{ \frac{5\omega[2n^3 - 5n(2n+\omega) + (2n^2+1)(2-\omega)] - 2(n-1)^2(n+1)[2-\omega]^2 - 2(2-\omega)(2n+\omega) - 4(2n+\omega)^2}{5(n+1)^{3/2}} \sqrt{\omega+n-1} \right\} \right]$$

$$\frac{3\omega^2}{2\sqrt{1-n^2}} \left[ \frac{\sin^{-1} \frac{2(n-1)+\omega}{\omega} - \sin^{-1} n}{\sqrt{1-n^2}} \right] + \frac{1}{\sqrt{1+n}} \left\{ \frac{3+7n+12\omega}{15} \sqrt{(\omega+n-1)^3} - \frac{(5n-3)(1+n) + \omega(9+5n)}{16\sqrt{2}} \left[ (3-n-\omega)\sqrt{2(\omega+n-1)} - \right. \right.$$

$$\left. \left. \frac{(1+n+\omega)^2}{2} \left( \sin^{-1} \frac{\omega+n-3}{\omega+n+1} + \frac{\pi}{2} \right) \right] \right\} \quad (15b)$$

Derivative  $C_{m_q}$ 

Consideration is now given to the damping-in-pitch derivative  $C_{m_q}$ . If the axis for pitching is located at the apex of the wing,  $C_{m_q}$  for the entire wing may be expressed as

$$C_{m_q} = (C_{m_q})_{ex} + (C_{m_q})_{in} + \Delta C_{m_q}$$

$$= - \frac{4V}{qSc^2} \iint_{\substack{\text{Regions} \\ \text{Ohg+Oge}}} x (C_{P_{ex}})_q dx dy - \frac{4V}{qSc^2} \iint_{\substack{\text{Region} \\ \text{egf}}} x (C_{P_{in}})_q dx dy +$$

$$\Delta C_{m_q} \tag{16}$$

The nondimensional pressures  $(C_{P_{ex}})_q$  and  $(C_{P_{in}})_q$  have already been determined for the evaluation of  $C_{L_q}$ . The expressions for these pressures are given by formulas (8) and (12), respectively. The term  $\Delta C_{m_q}$  is the approximate subsonic-edge correction for pitching and is evaluated in reference 13. Substitution of the pressure coefficients of equations (8) and (12) into equation (16) together with a consideration of the limits of integration (fig. 3(b)) allows equation (16) to be expressed in the following integral form:



$$C_{mq} = - \frac{4\theta_0^2 G(m) c_r^4}{S c^2} \int_0^{\frac{1-\omega+m}{(1+m)n+\omega n}} \frac{(2-v^2)dv}{(1-nv)^4 \sqrt{1-v^2}} - \frac{G(m)(1+m)b^4}{4S c^2 \theta_0^2} \int_0^1 \frac{(2-v^2)dv}{(1+mv)^4 \sqrt{1-v^2}}$$

$$\frac{16}{3\pi S c^2} \int_{b/2}^{b/2} \frac{b(1+m-\omega)}{2(n+m)} \int_{b(1+m)-By}^{c_r+\theta_0} \frac{ny}{\theta_0} \sqrt{\frac{(b-2y)(1+m)}{2(\theta_0 x + y)}} \left[ \frac{6\theta_0 x(3+2m) + y(12+8m+2m^2) - bm(1+m)}{(1+m)^2} \right] x \, dx \, dy +$$

$$\left( \frac{48m^3 G(m) \omega^2}{\left[ 3\omega^2 - 3\omega(1-n) + (1-n)^2 \right]^2 AB^2} \left\{ \left[ 1 - \frac{\pi}{2K'(g)} \right] + \frac{n}{\omega} \left[ 2 - \frac{E'(g)}{K'(g)} - \frac{E'(g)}{K'(g)} - \frac{E'^2(g)}{E'(g)} \right] \right\} + \frac{n^2}{2\omega^2} \left[ 1 - \frac{\pi}{4} \frac{1-g^2}{K'(g) - E'(g)} \right] \right) \quad (17)$$

The first and second integrals of equation (17) pertain to the contribution of the region of the wing external to the wing-tip Mach cones to the pitching derivative. The third integral term is the contribution of the wing-tip region and the remaining terms obtained from reference 13 give the subsonic trailing-edge correction for pitching about the apex of the wing. Evaluation of the integrals in equation (17) affords the following equation for the derivative  $C_{mq}$  for pitching motion about the apex of the wing:



## RESULTS AND DISCUSSION

On the basis of the linearized supersonic-flow theory the foregoing analysis resulted in the evaluation of the longitudinal-stability derivatives  $C_{m_\alpha}$ ,  $C_{L_q}$ , and  $C_{m_q}$  for a series of sweptback tapered wings.

For the evaluation of the derivative  $C_{m_\alpha}$ , the pressure distribution for the region of the wing external to the wing-tip Mach cones was obtained from reference 4 and the approximate subsonic-edge correction for the trailing-edge region, from reference 7. For the wing-tip regions, the expression for the approximate lift pressure given in reference 8 was used. Previous to that investigation an exact linearized solution of the pressure for the wing-tip region was presented in reference 7. This exact solution, however, inherently complicated because of the nonconical boundary defining the wing-tip region, did not lend itself readily to practical evaluations of  $C_{m_\alpha}$  for families of wings. The comparison of the approximate and exact pressure distributions for the wing-tip region made in reference 8 and the comparison of the approximate and exact subsonic-edge correction for angle of attack made in reference 7 indicate the satisfactory accuracy of these approximations relative to the exact linearized formulations.

In regard to the lift and the damping-in-pitch derivatives  $C_{L_q}$  and  $C_{m_q}$ , the expression for the pressure due to pitching for the region of the wing external to the wing-tip Mach cones and for the trailing-edge region was obtained directly from reference 5. The exact linearized solution for the lifting pressure in the wing-tip region and in the trailing-edge region is not available at present, although extremely accurate approximations to the exact linearized solutions that require laborious calculations may be obtained by the methods of reference 15. On this basis, resort was made herein to the relatively simple but less accurate procedure for the evaluation of the lifting pressure in the wing-tip region considered in reference 8. For the trailing-edge region, the simple approximate corrections for the effect of the subsonic trailing-edge disturbances reported in reference 13 were used. For a typical wing pitching about its apex, figure 5 gives the chordwise and spanwise lifting-pressure distributions along sections through the wing-tip region. A situation is noted to exist for pitching analogous to the angle-of-attack case in regard to the relatively small positive residual pressure in the wing-tip region demanded by the large finite drop in pressure across the inboard Mach line from the wing tip. The pressure distributions of figure 5 indicate the inadequacy of the approximate subsonic trailing-edge correction in properly altering the basic lifting pressure in the subsonic trailing-edge region so that the Kutta condition is satisfied along the trailing edge. Additional

corrections must be considered in order to bring the perturbed flow pressure to zero along this edge. The qualitative effect of the uncorrected negative pressure in the vicinity of the trailing edge is to reduce the positive lift due to pitching  $CL_q$  and to decrease the damping due to pitching  $Cm_q$ . In an attempt to ascertain the magnitude of the errors involved in the approximate formulas for  $CL_q$  and  $Cm_q$ , calculations were prepared based upon conservative estimates of the additional corrections necessary to obtain the true linearized pressure in the subsonic trailing-edge region. For the Mach number range considered herein and for a static margin,  $\frac{\partial C_m}{\partial C_L} = 0.05$ , the results of these calculations indicate that the derivative  $CL_q$  may be in error as much as 8 percent and the derivative  $Cm_q$ , as much as 12 percent. A precise evaluation of the magnitude of the errors involved cannot be made until the exact solutions are determined for the pressure in the wing-tip and subsonic trailing-edge regions.

A series of generalized curves that allow rapid estimations of the derivatives  $Cm_\alpha$ ,  $CL_q$ , and  $Cm_q$  are presented in figures 6, 7, and 8, respectively, for specified values of aspect ratio, taper ratio, Mach number, and leading-edge sweep. The variation of these curves with  $B \cot \Lambda$  requires additional emphasis because of the various critical locations of the Mach lines relative to the wing. The point of discontinuity of each curve represents the configuration for which the Mach lines from the apex of the trailing edge coincides with the trailing edge of the wing. The parts of the curves to the right of the points of discontinuity give the values of the derivatives when the trailing edge is supersonic (Mach lines behind trailing edge). The segments of the curves between the point of discontinuity and the boundary line give the values of the derivatives when the trailing edge is subsonic (Mach lines ahead of the trailing edge). The remnant parts of the curves to the left of the boundary curve should be disregarded for estimations; they correspond to the condition not treated in this paper for which the trailing-edge disturbance affects the leading edge of the wing (Mach lines intersect leading edge). The dashed parts of the curves have been presented, however, to indicate the trend of the variations and, for the segments shown, to act as an upper limit below which the true values of the derivatives would lie for configurations where the Mach lines from the apex of the trailing edge would intersect the leading edge of the wing.

It should be carefully noted that the derivatives given by these generalized curves are for the wing pitching about its apex. The derivatives with respect to an arbitrary center-of-gravity location ( $x = \bar{x}$ ,  $y = 0$ ,  $z = 0$ ) may be obtained by the transformation formulas (reference 16) presented in table 1. The first column of table 1 comprises

the derivatives in the body axes system with respect to the origin at the apex of the wing (0,0,0). In the second column, the derivatives in the body axes system with respect to the origin at an arbitrary center-of-gravity location ( $\bar{x}$ ,0,0) are presented. In the third column, the derivatives in the stability axes system with respect to the origin ( $\bar{x}$ ,0,0) are presented. Briefly then, the second column allows a translation of the origin to be made from  $x = 0$ ,  $y = 0$ ,  $z = 0$  to  $x = \bar{x}$ ,  $y = 0$ ,  $z = 0$  and the third column, a pitch of the axes through an angle  $\alpha$  about the lateral axis through the arbitrary center-of-gravity location ( $\bar{x}$ ,0,0).

It should be noted from table 1 that the lift-curve slope  $CL_\alpha$  must be known in order to translate the origin. For this reason a series of design curves for  $CL_\alpha$  have been prepared and are presented in figure 9 for the range of Mach number and geometric wing parameters considered for the pitching derivatives. The parts of these curves that correspond to wings with subsonic leading edges and supersonic trailing edges were obtained directly from reference 8 for taper ratios of 0.25 and 0.50. The parts of the curves that correspond to wings with subsonic trailing edges were determined by an application of the appropriate approximate subsonic trailing-edge correction for angle of attack that was reported in reference 7.

Specific variations of the derivatives (in the stability axes system)  $C_{m_\alpha}$ ,  $CL_q$ , and  $C_{m_q}$  with each of the parameters - aspect ratio, taper ratio, Mach number, and leading-edge sweep - are presented in figures 10, 11, and 12, respectively.

#### CONCLUDING REMARKS

On the basis of linearized supersonic-flow theory, approximations to the static-pitching derivative  $C_{m_\alpha}$ , the lift-due-to-pitching derivative  $CL_q$ , and the damping-in-pitch derivative  $C_{m_q}$  were derived for a series of thin sweptback tapered wings with streamwise tips and subsonic leading edges. The applicability of the expressions determined for the derivatives should be satisfactory if their approximations to the corresponding exact linearized evaluations are considered as a criterion (for cases where a comparison could be made). The suitability of the results for full-scale flight stability calculations is necessarily limited because of the restrictions of the linearized

potential-flow theory together with the additional simplifying assumptions that the wing has vanishingly small thickness and zero camber.

Langley Aeronautical Laboratory  
National Advisory Committee for Aeronautics  
Langley Field, Va., November 24, 1950

## APPENDIX

EVALUATION OF APPROXIMATE EQUATION FOR SURFACE  
VELOCITY POTENTIAL FOR PITCHING

The integral equation for the approximate surface velocity potential of a lifting wing was derived in reference 8 and may be expressed as (refer to fig. 3(a))

$$\phi = \frac{V}{\pi} \iint_{S_{W,0}} \frac{\alpha(\xi, \eta) d\xi d\eta}{\sqrt{(x - \xi)^2 - B^2(y - \eta)^2}} \quad (A1)$$

For the wing undergoing a steady pitching motion about a lateral axis located at the apex of the wing, the local angle of attack  $\alpha(\xi, \eta)$  becomes equal to  $q\xi/V$  where the quantity  $q\xi$  is the local downwash due to pitching. Substitution of  $q\xi/V$  for  $\alpha(\xi, \eta)$  in equation (A1) gives the following equation for the approximate surface velocity potential for pitching about the apex of the wing:

$$(\phi)_q = \frac{q}{\pi} \iint_{S_{W,0}} \frac{\xi d\xi d\eta}{\sqrt{(x - \xi)^2 - B^2(y - \eta)^2}} \quad (A2)$$

The integral of equation (A2) is readily evaluated by the use of an oblique  $u, v$ -coordinate system, the axes of which are coincident with the Mach lines from the apex of the wing. (See reference 14.) The transformation equations are

$$\left. \begin{aligned} u &= \frac{M}{2B}(\xi - B\eta) \\ v &= \frac{M}{2B}(\xi + B\eta) \\ \xi &= \frac{B}{M}(u + v) \\ \eta &= \frac{1}{M}(v - u) \end{aligned} \right\} \quad (A3)$$

Appropriate use of transformations of equations (A3) allows equation (A2) to be expressed as

$$(\phi)_q = \frac{Bq}{\pi M^2} \iint_{S_{W,0}} \frac{(u + v) du dv}{\sqrt{(u_w - u)(v_w - v)}} \quad (A4)$$

where  $u_w$  and  $v_w$  are the coordinates of a field point and are related to the corresponding  $x, y$  field point as follows:

$$u_w = \frac{M}{2B}(x - By)$$

$$v_w = \frac{M}{2B}(x + By)$$

The limits in integration defined by the region  $S_{W,0}$  are given in figure 3(a) and the potential function of equation (A4) may now be expressed as

$$(\phi)_q = \frac{Bq}{\pi M^2} \int_{\frac{1-m}{1+m}u_w}^{v_w} \left[ \int_{v_w - \frac{bM}{2}}^{u_w} \frac{(v + u) du}{\sqrt{u_w - u}} \right] \frac{dv}{\sqrt{v_w - v}} \quad (A5)$$

Integration of equation (A5) yields

$$(\phi)_q = \frac{4Bq}{3\pi M^2} \left\{ 3v_w + u_w \left( \frac{1-m}{1+m} + 2 \right) - \frac{bM}{2} \sqrt{\left( v_w - \frac{1-m}{1+m} u_w \right) \left( u_w - v_w + \frac{bM}{2} \right)} \right\} \quad (A6)$$

Equation (A6) transformed into  $x, y$ -coordinates becomes

$$(\phi)_q = \frac{q}{3\pi B(1+m)^{3/2}} \left\{ 2x(3+2m) + 2mBy - bB(1+m) \right\} \sqrt{(2B(mx + By)(b - 2y))} \quad (A7)$$

and is given as equation (11) in the main body of the paper.



## REFERENCES

1. Harmon, Sidney M.: Stability Derivatives at Supersonic Speeds of Thin Rectangular Wings with Diagonals ahead of Tip Mach Lines. NACA Rep. 925, 1949.
2. Ribner, Herbert S., and Malvestuto, Frank S., Jr.: Stability Derivatives of Triangular Wings at Supersonic Speeds. NACA Rep. 908, 1948.
3. Malvestuto, Frank S., Jr., and Margolis, Kenneth: Theoretical Stability Derivatives of Thin Sweptback Wings Tapered to a Point with Sweptback or Sweptforward Trailing Edges for a Limited Range of Supersonic Speeds. NACA Rep. 971, 1950.
4. Brown, Clinton E.: Theoretical Lift and Drag of Thin Triangular Wings at Supersonic Speeds. NACA Rep. 839, 1946.
5. Brown, Clinton E., and Adams, Mac C.: Damping in Pitch and Roll of Triangular Wings at Supersonic Speeds. NACA Rep. 892, 1948.
6. Jones, Arthur L., and Alksne, Alberta: The Damping Due to Roll of Triangular, Trapezoidal, and Related Plan Forms in Supersonic Flow. NACA TN 1548, 1948.
7. Cohen, Doris: The Theoretical Lift of Flat Sweptback Wings at Supersonic Speeds. NACA TN 1555, 1948.
8. Malvestuto, Frank S., Jr., Margolis, Kenneth, and Ribner, Herbert S.: Theoretical Lift and Damping in Roll at Supersonic Speeds of Thin Sweptback Wings with Streamwise Tips, Subsonic Leading Edges, and Supersonic Trailing Edges. NACA Rep. 970, 1950.
9. Harmon, Sidney M., and Jeffreys, Isabella: Theoretical Lift and Damping in Roll of Thin Wings with Arbitrary Sweep and Taper at Supersonic Speeds. Supersonic Leading and Trailing Edges. NACA TN 2114, 1950.
10. Walker, Harold J., and Ballantyne, Mary B.: Pressure Distribution and Damping in Steady Roll at Supersonic Mach Numbers of Flat Swept-Back Wings with Subsonic Edges. NACA TN 2047, 1950.
11. Harmon, Sidney M., and Martin, John C.: Theoretical Calculations of the Lateral Force and Yawing Moment Due to Rolling at Supersonic Speeds for Sweptback Tapered Wings with Streamwise Tips. Supersonic Leading Edges. NACA TN 2156, 1950.

12. Margolis, Kenneth: Theoretical Calculations of the Lateral Force and Yawing Moment Due to Rolling at Supersonic Speeds for Swept-back Tapered Wings with Streamwise Tips. Subsonic Leading Edges. NACA TN 2122, 1950.
13. Ribner, Herbert S.: On the Effect of Subsonic Trailing Edges on Damping in Roll and Pitch of Thin Sweptback Wings in a Supersonic Stream. NACA TN 2146, 1950.
14. Evvard, John C.: Theoretical Distribution of Lift on Thin Wings at Supersonic Speeds (An Extension). NACA TN 1585, 1948.
15. Mirels, Harold: Lift-Cancellation Technique in Linearized Supersonic-Wing Theory. NACA TN 2145, 1950.
16. Glauert, H.: A Non-Dimensional Form of the Stability Equations of an Aeroplane. R. & M. No. 1093, British A.R.C., 1927.

TABLE 1.- TRANSFORMATION FORMULAS FROM BODY AXES TO STABILITY AXES FOR

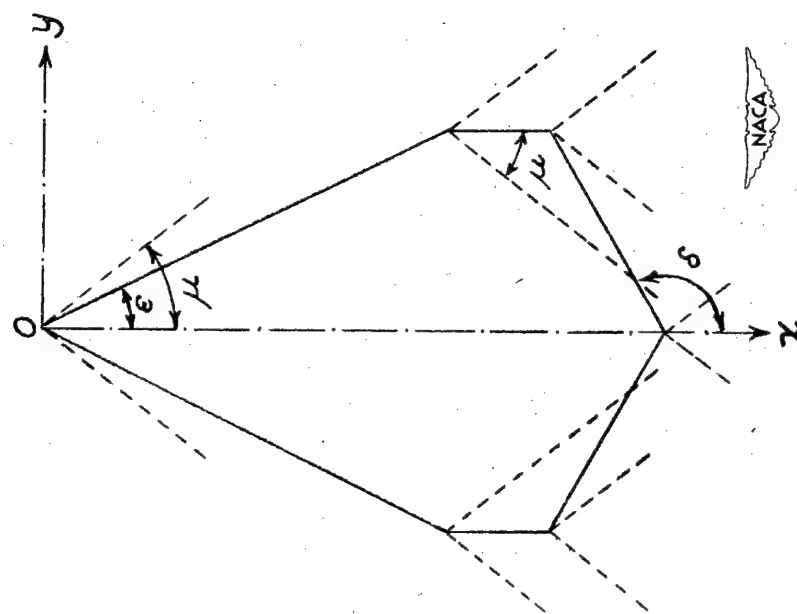
STABILITY DERIVATIVES  $C_{m_\alpha}$ ,  $C_{L_q}$ , AND  $C_{m_q}$ 

Principal body axes (origin at $x = 0, y = 0, z = 0$ )	Principal body axes (origin at $x = x, y = 0, z = 0$ )		Stability axes (origin at $x = x, y = 0, z = 0$ )	
	Stability derivative	Shift in origin from (0,0,0) to ( $\bar{x}$ ,0,0)	Stability derivative (2)	Origin at ( $\bar{x}$ ,0,0); rotation through angle $\alpha$
$C_{m_\alpha}$	$C_{m_\alpha}'$	$C_{m_\alpha} + \frac{\bar{x}}{c} C_{L_\alpha}$	$C_{m_\alpha}''$	$C_{m_\alpha}' - \alpha C_{m_u}' \approx C_{m_\alpha}'$
$C_{L_q}$	$C_{L_q}'$	$C_{L_q} - 2\frac{\bar{x}}{c} C_{L_\alpha}$	$C_{L_q}''$	$C_{L_q}' - \alpha C_{x_q}' \approx C_{L_q}'$
$C_{m_q}$	$C_{m_q}'$	$C_{m_q} - \frac{\bar{x}}{c} (-C_{L_q} + 2C_{m_\alpha}) - 2\frac{\bar{x}^2}{c^2} C_{L_\alpha}$	$C_{m_q}''$	$C_{m_q}'$

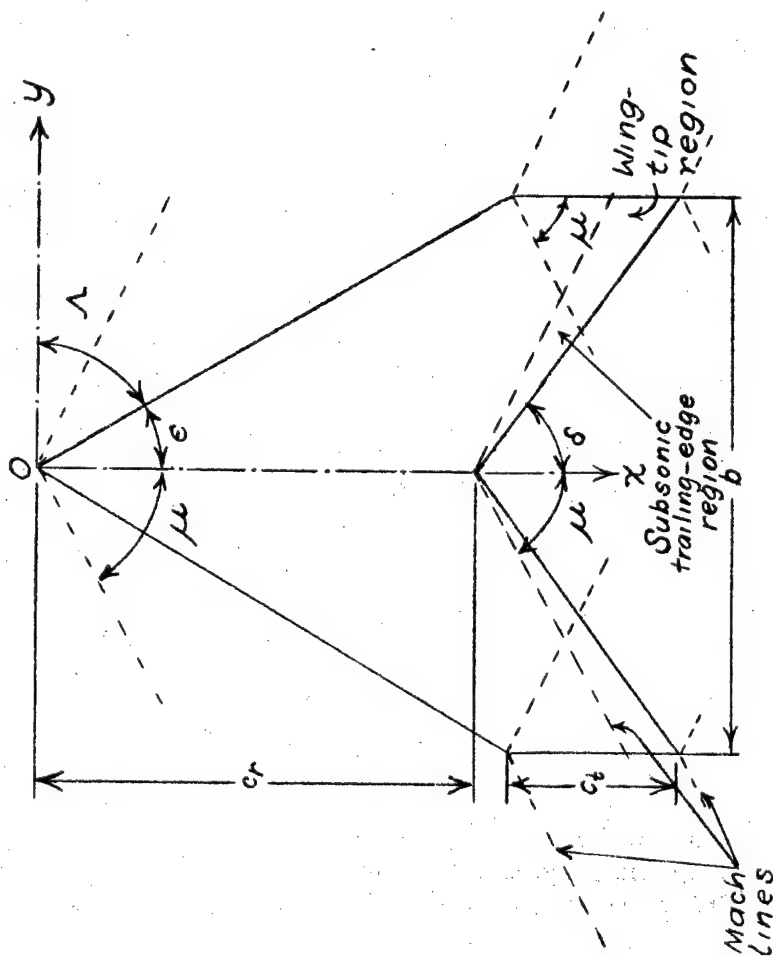
<sup>1</sup>The values of the stability derivatives in this column (origin at (0,0,0)) are obtained from figures 6 to 8 or from formulas (7), (15), and (18).

<sup>2</sup>The value of  $\alpha C_{m_u}'$  in the transformation for  $C_{m_\alpha}''$  and the value of  $\alpha C_{x_q}'$  in the transformation for  $C_{L_q}''$  are of second order in  $\alpha$  and may be disregarded for estimations of  $C_{m_\alpha}''$  and  $C_{L_q}''$ . These values have not been evaluated in this paper.





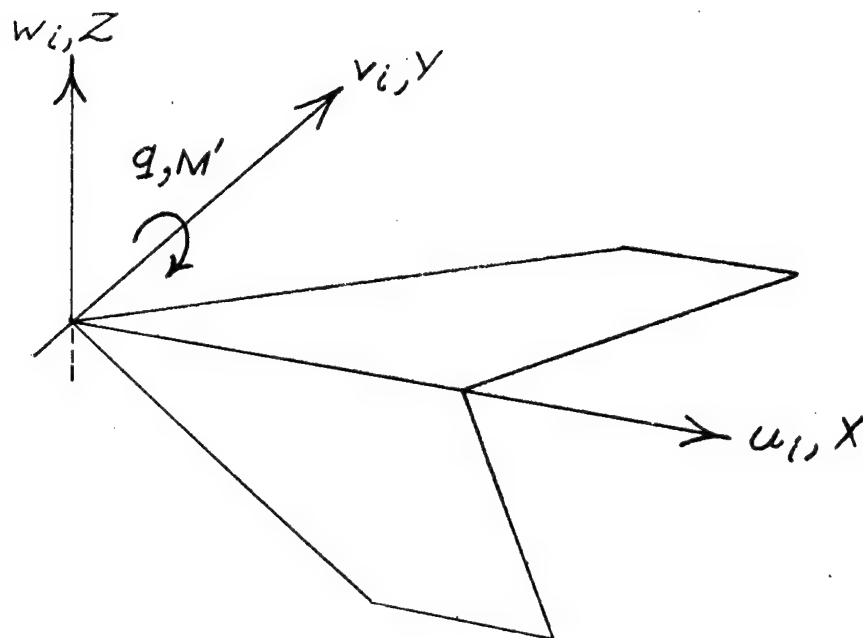
(b) Sweptforward trailing edge.



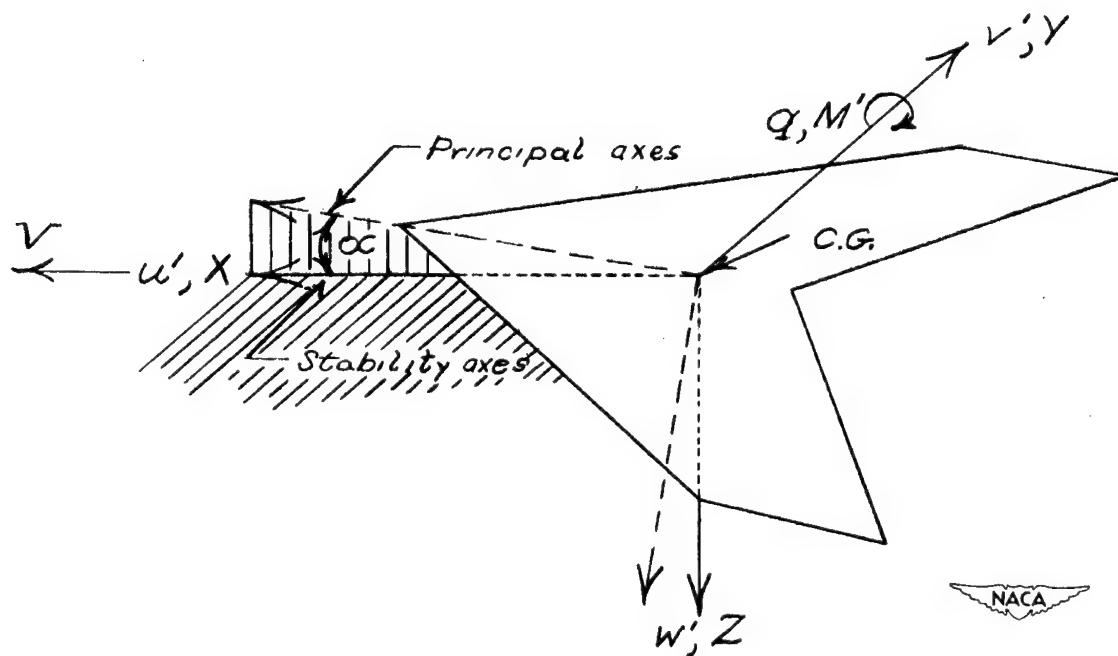
(a) Sweptback trailing edge.

Figure 1.- Sweptback wing with streamwise tips and sweptback or swept-forward trailing edges.



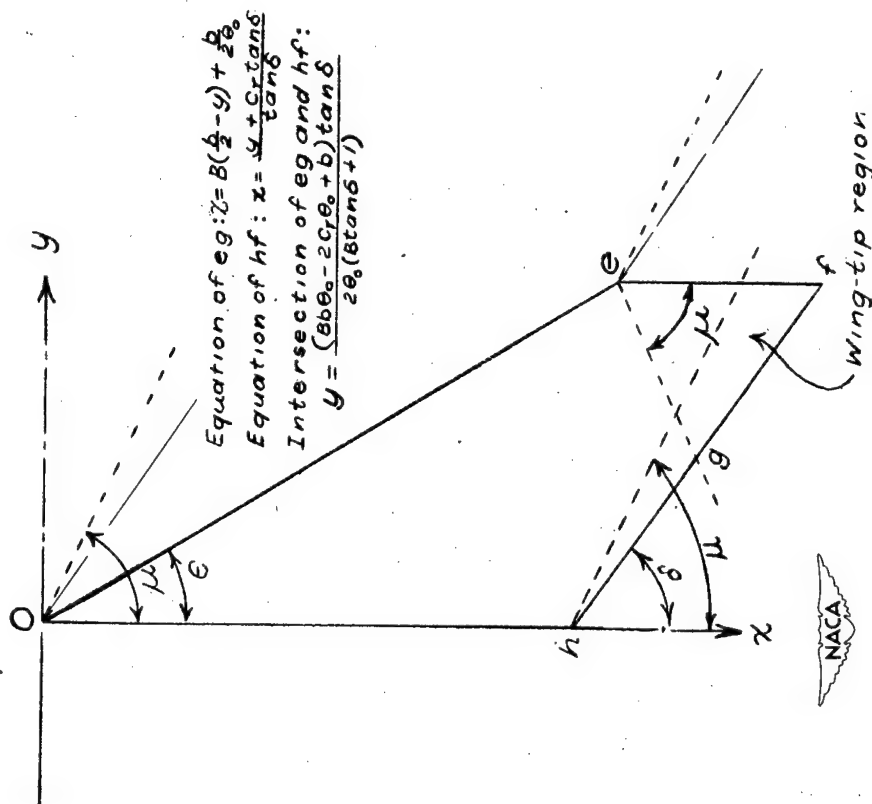


(a) Notation and body axes used in analysis.

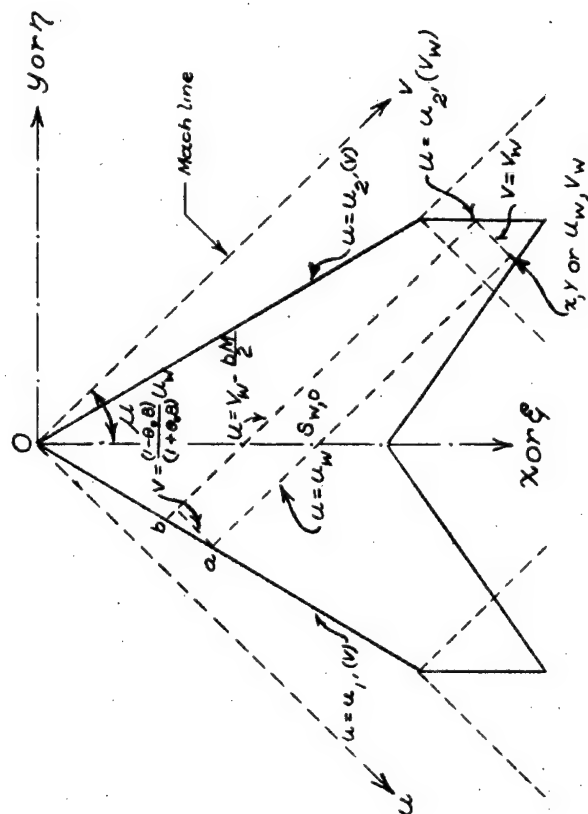


(b) Stability axes. Velocity, force, and moment arrangement in principal body axes system is the same as that of stability axes system. (Principal body axes dashed in for comparison.)

Figure 2.- System of axes and associated data.



(b) Equations of boundary lines defining limits of integration for evaluation of forces and moments.



(a) Area  $S_{w,0}$  for evaluation of surface velocity potential for angle of attack and pitching.

Figure 3.- Sketch of wing and associated data for the evaluation of the surface velocity potentials, forces, and moments.

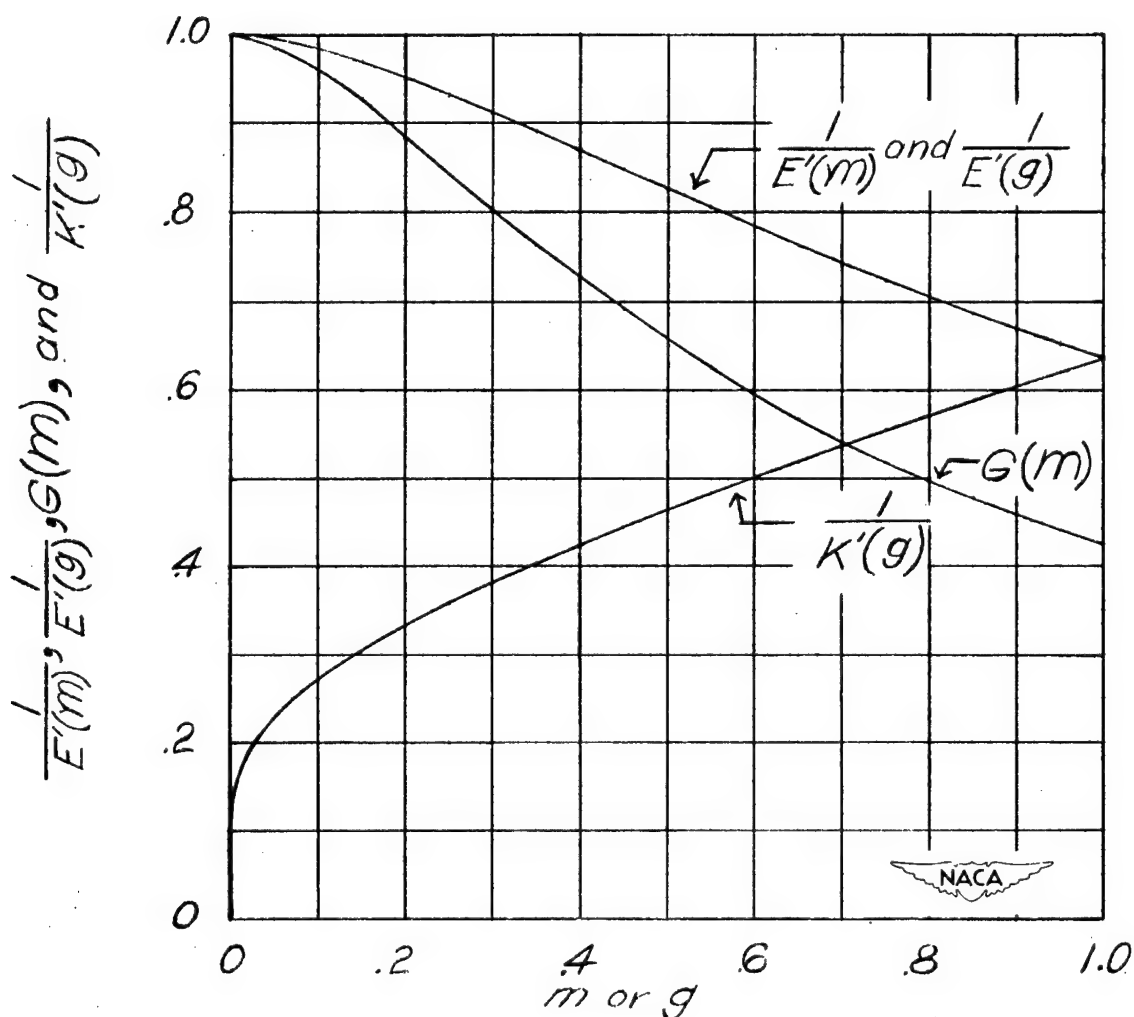
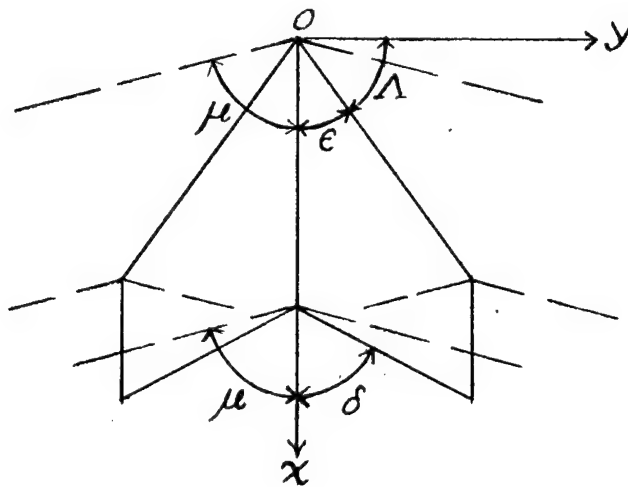


Figure 4.- Variation of elliptic integrals and factors with  $m = B \cot \Lambda$  and  $g = B \cot \delta$ .

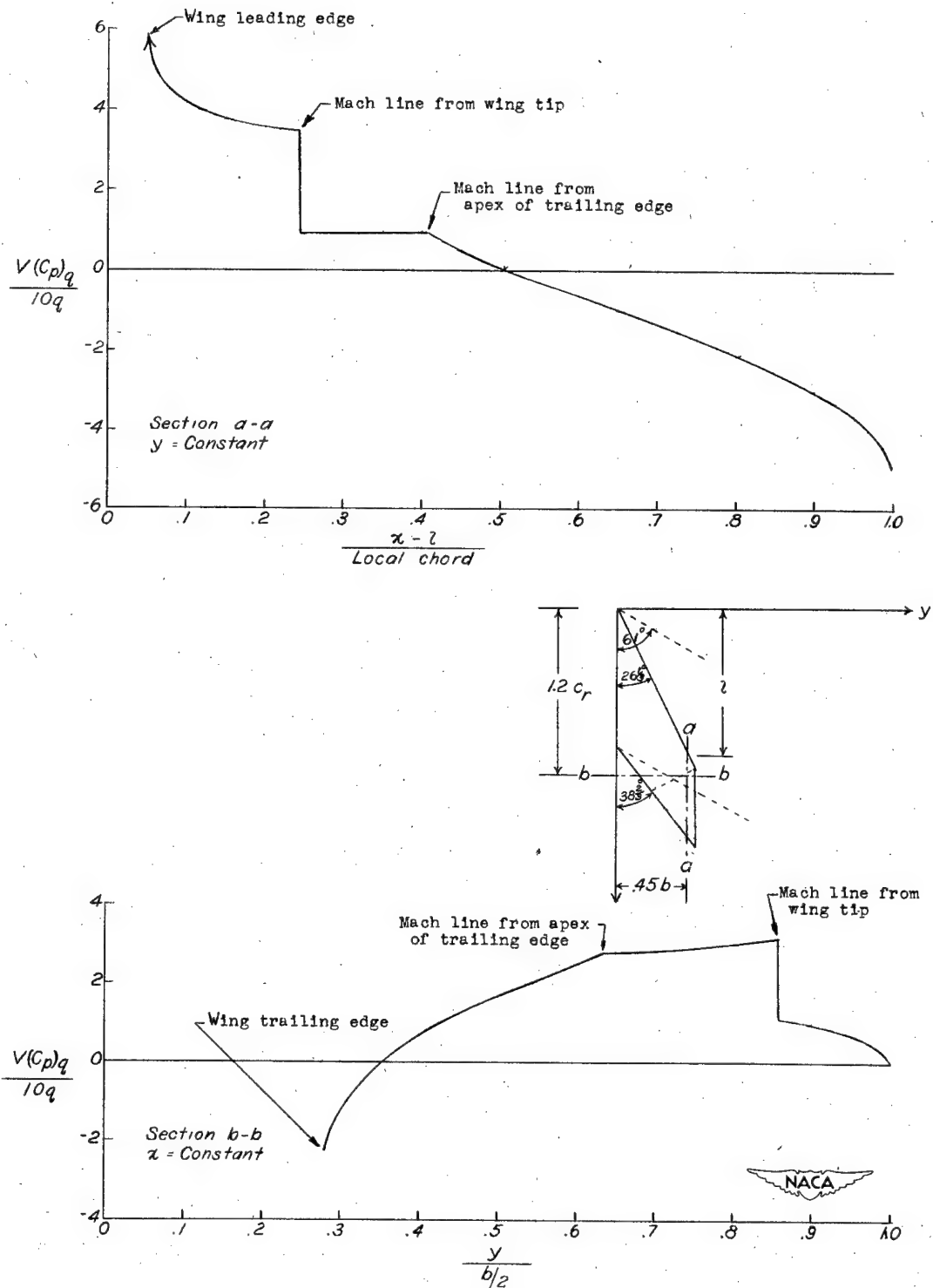


Figure 5.- Sectional chordwise and spanwise pressure distributions for a typical wing pitching about its apex. Intersection of the sectional planes a-a and b-b with the wing edges and Mach lines are noted on pressure curves.



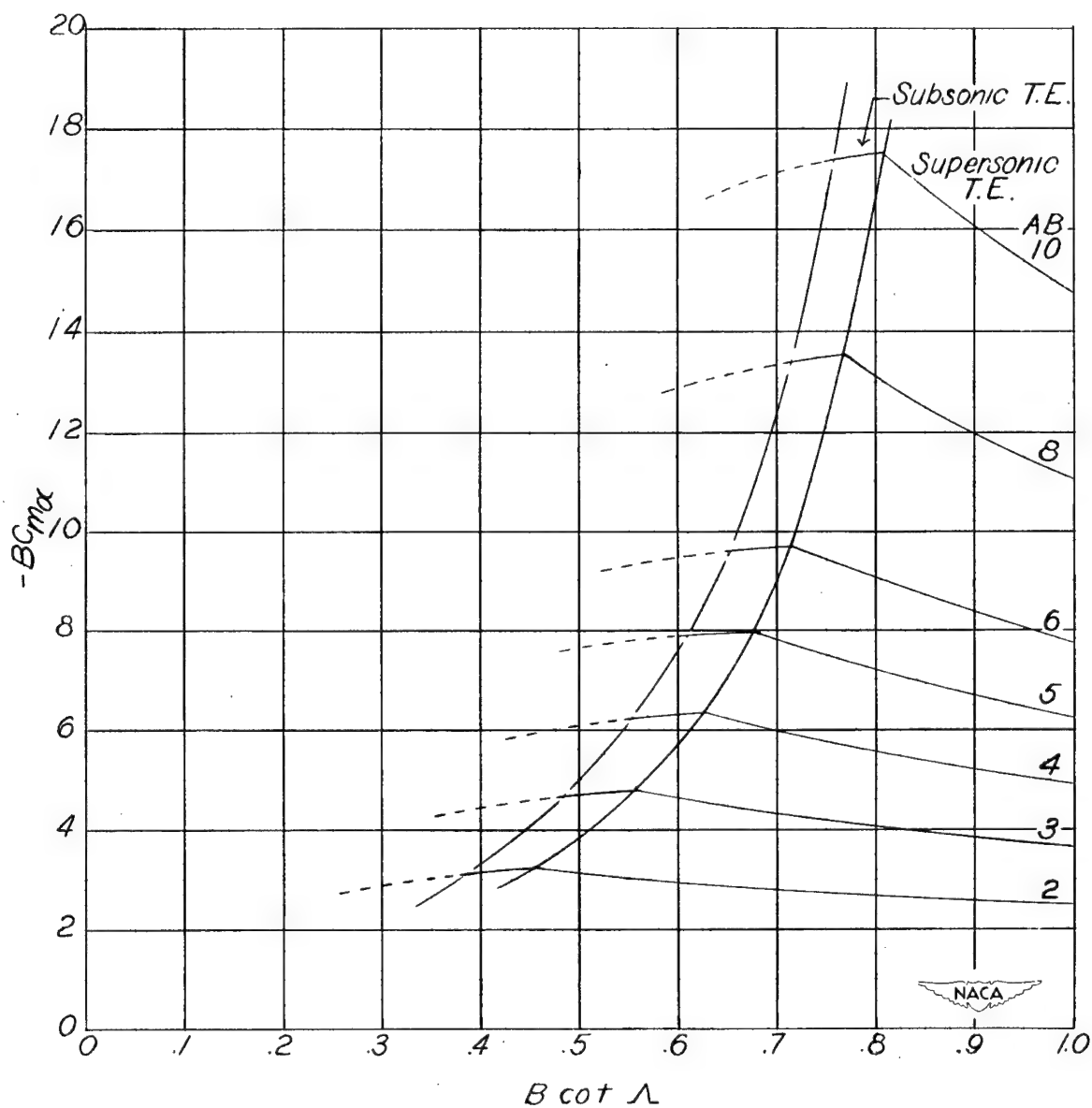
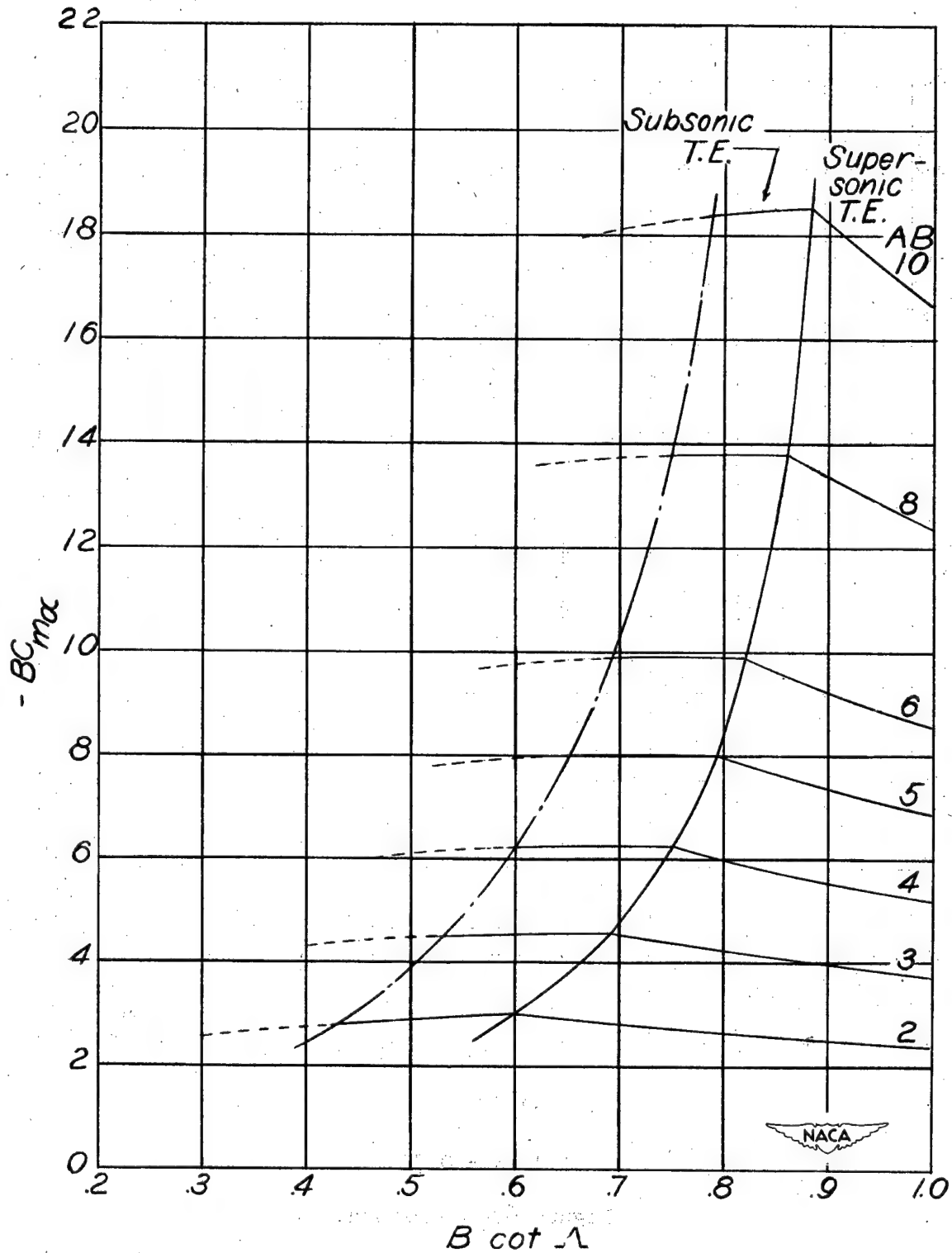
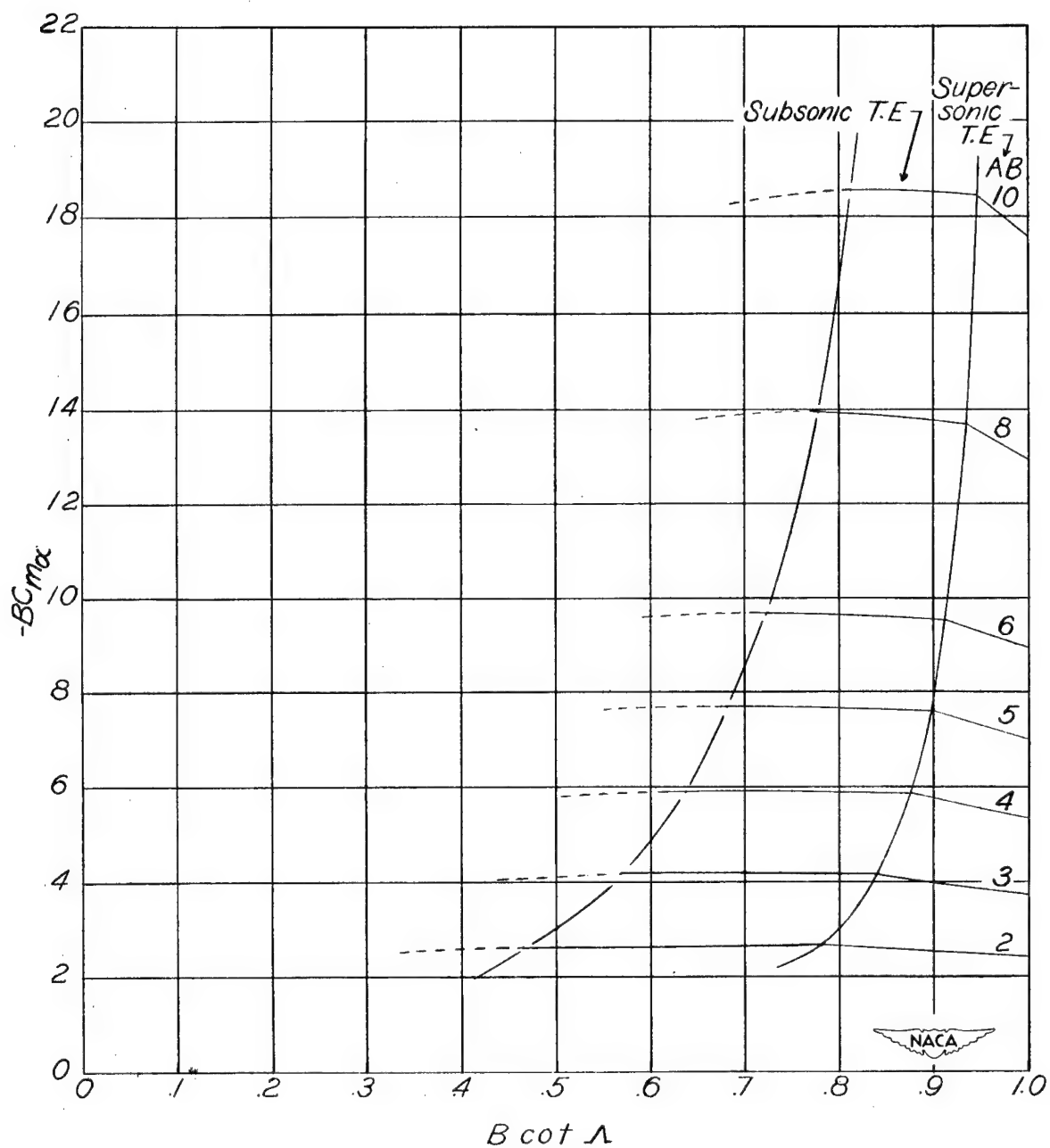
(a)  $\lambda = 0.25$ .

Figure 6.- Variation of  $BC_{m\alpha}$  with  $B \cot \Lambda$  for various values of  $BA$  and  $\lambda$ . Body axes system; origin at apex of wing. Dashed parts of curves have limited significance. (See section entitled "Results and Discussion.")



(b)  $\lambda = 0.50$ .

Figure 6.- Continued.



(c)  $\lambda = 0.75$ .

Figure 6.- Concluded.

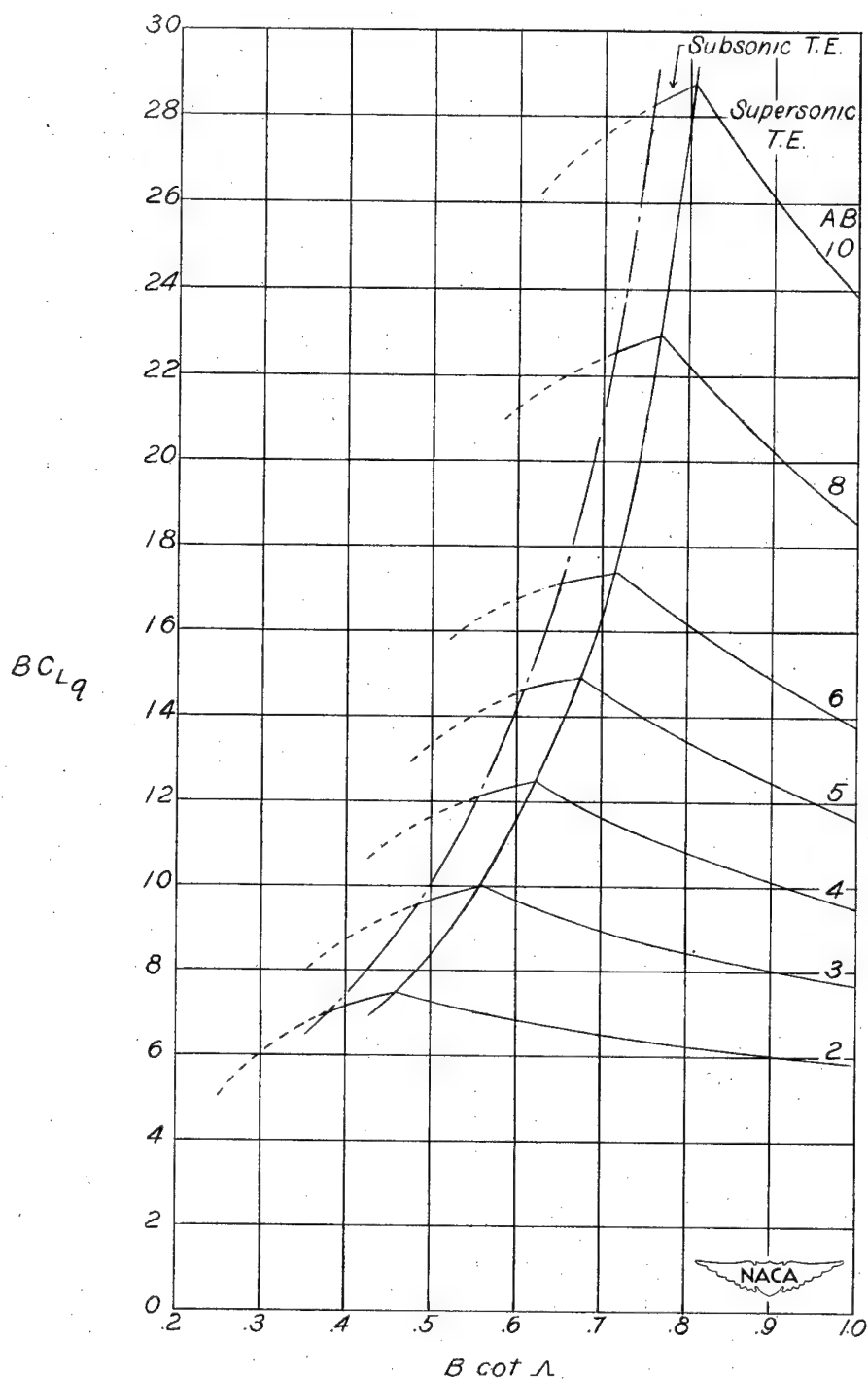
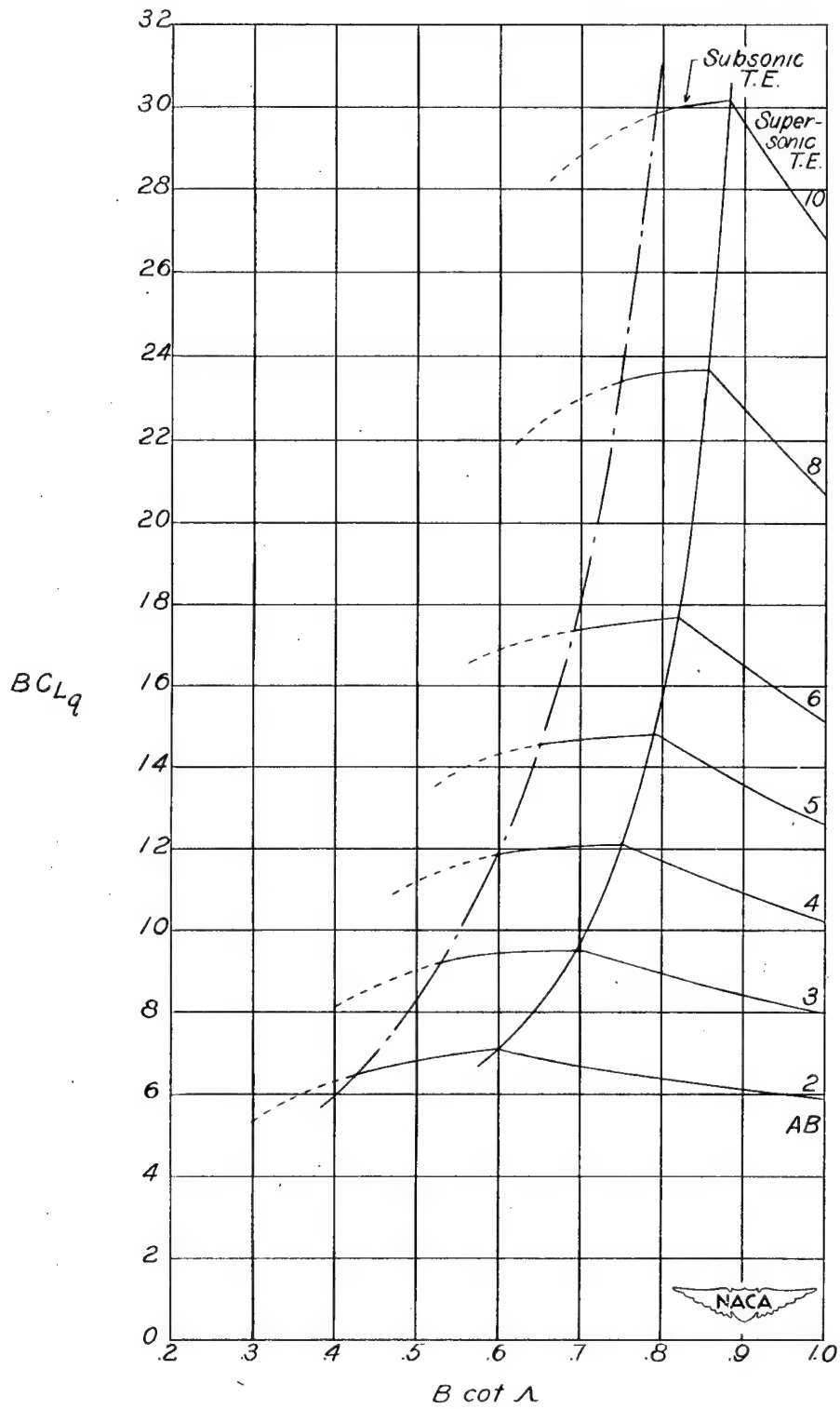
(a)  $\lambda = 0.25$ .

Figure 7.- Variation of  $BC_{Lq}$  with  $B \cot \Lambda$  for various values of  $BA$  and  $\lambda$ . Body axes system; origin at apex of wing. Dashed parts of curves have limited significance. (See section entitled "Results and Discussion.")



(b)  $\lambda = 0.50$ .

Figure 7.- Continued.

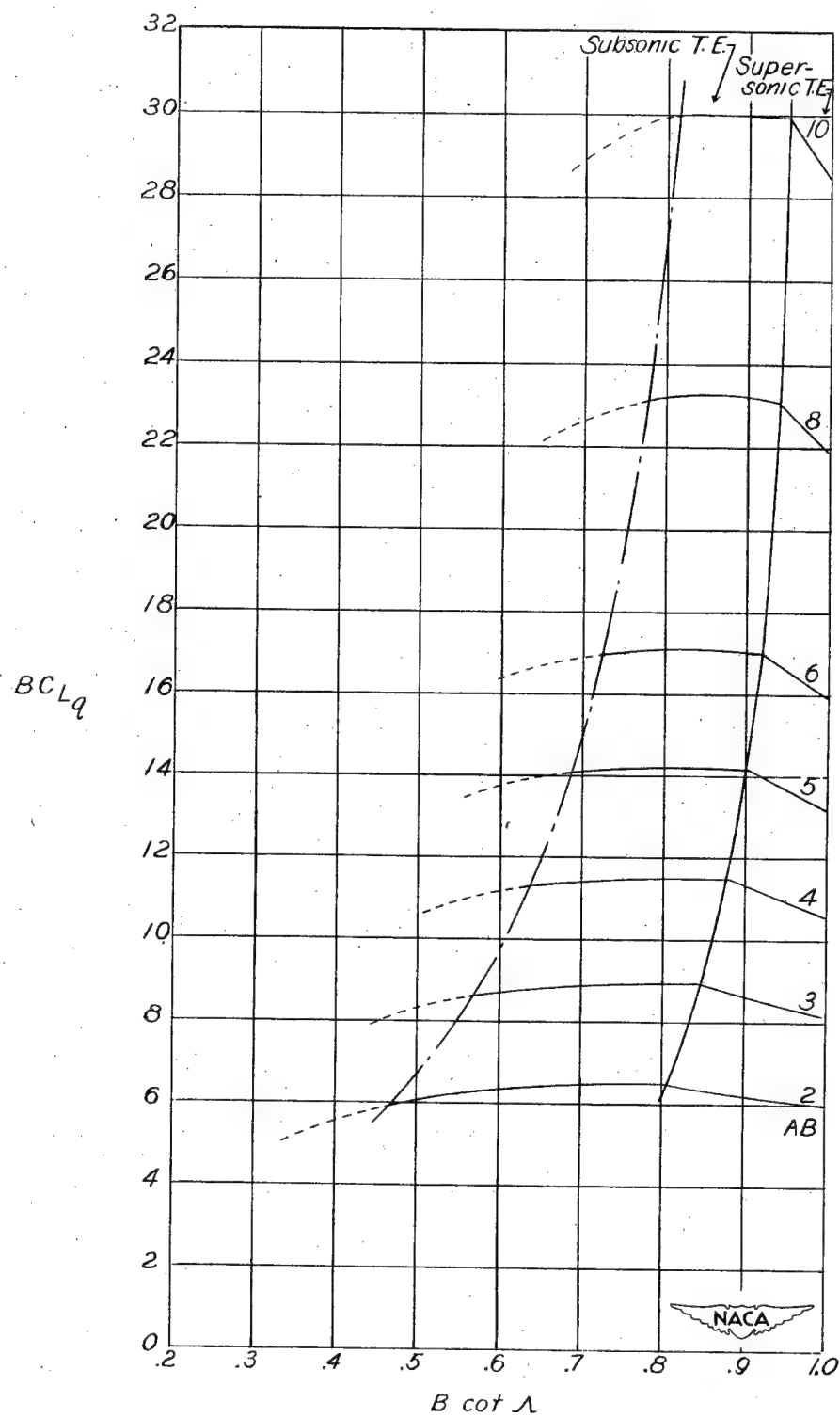
(c)  $\lambda = 0.75$ .

Figure 7.- Concluded.

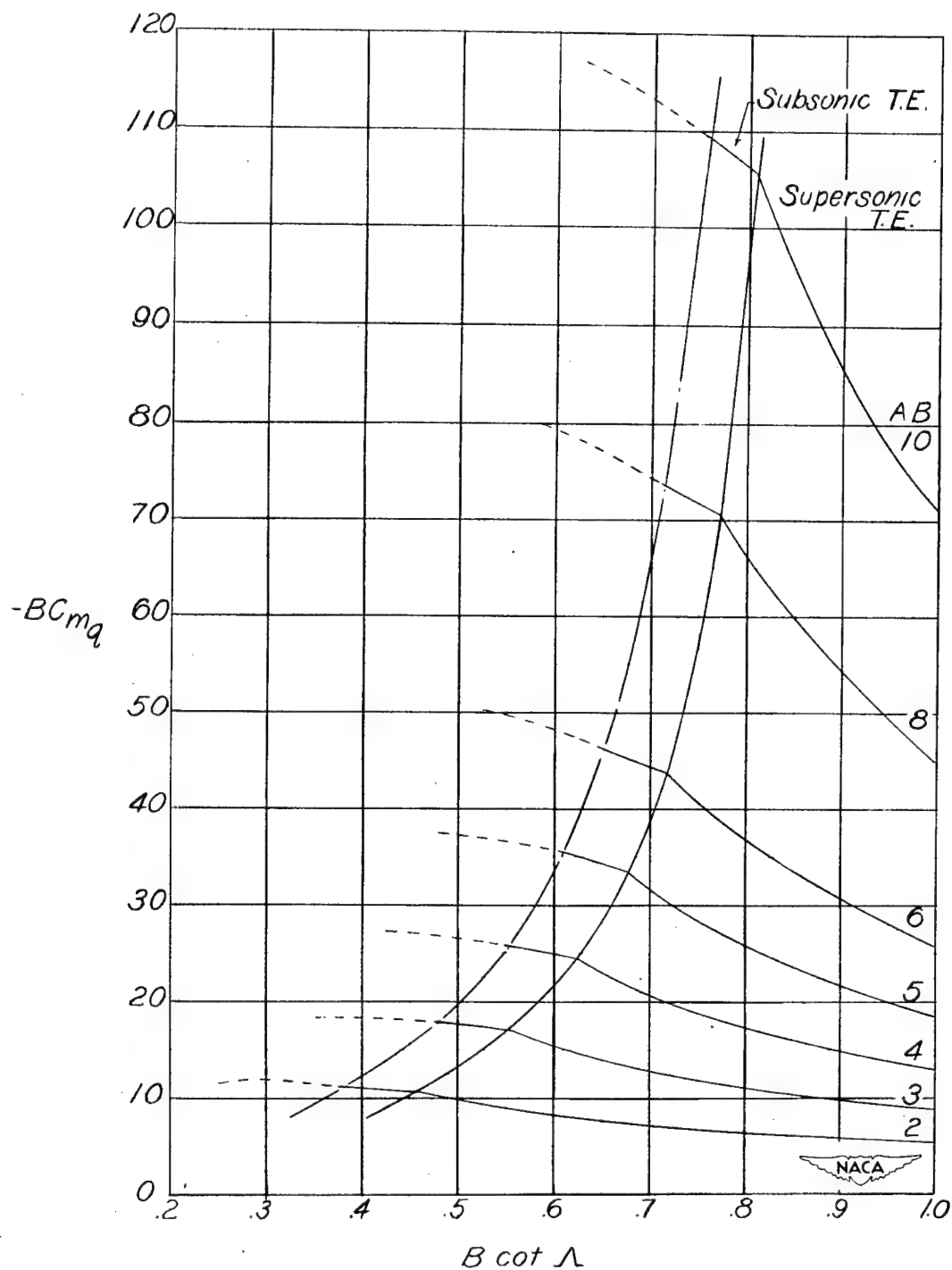
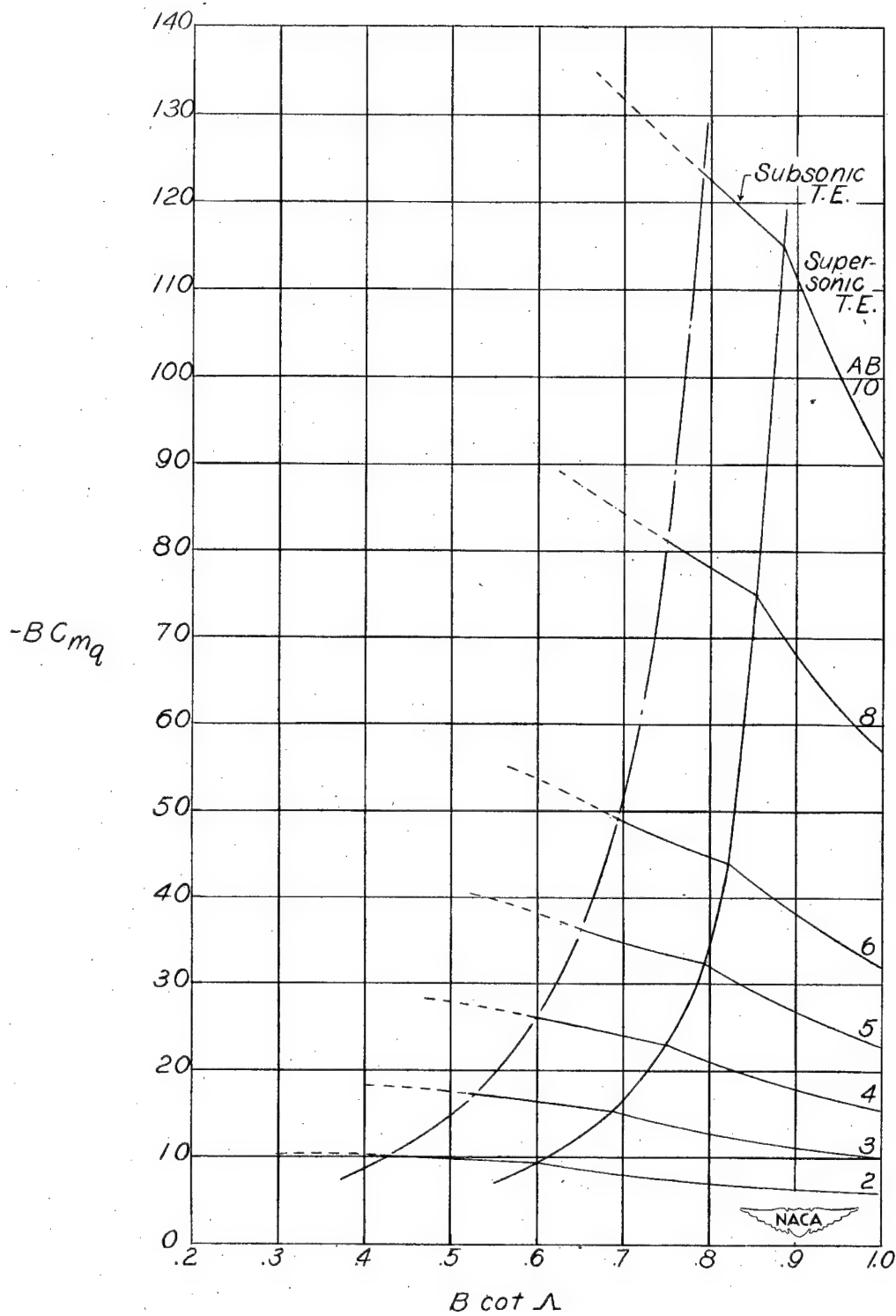
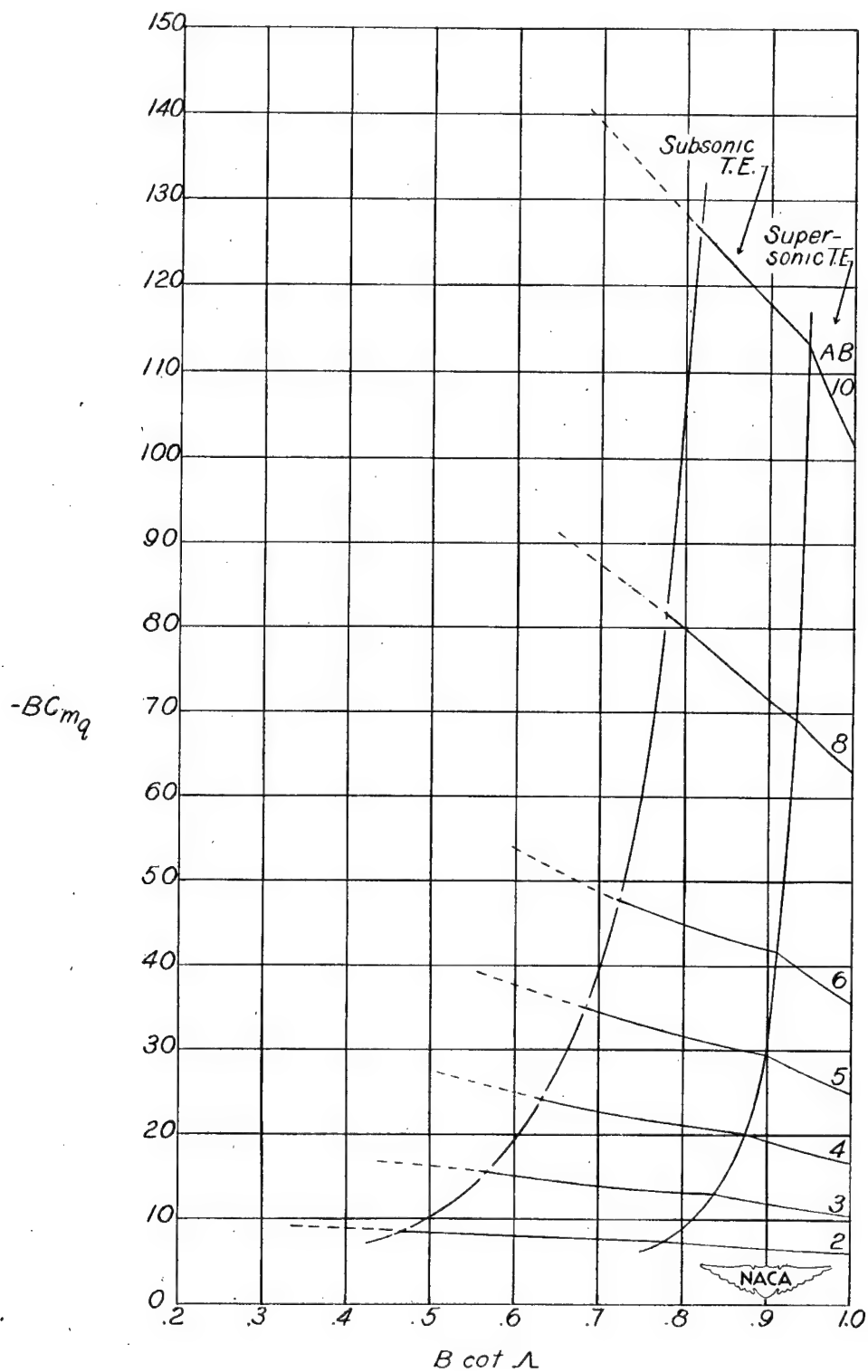
(a)  $\lambda = 0.25$ .

Figure 8.- Variation of  $BC_{mq}$  with  $B \cot \Lambda$  for various values of  $BA$  and  $\lambda$ . Body axes system; origin at apex of wing. Dashed parts of curves have limited significance. (See section entitled "Results and Discussion.")



(b)  $\lambda = 0.50$ .  
Figure 8.- Continued.





(c)  $\lambda = 0.75$ .

Figure 8.- Concluded.

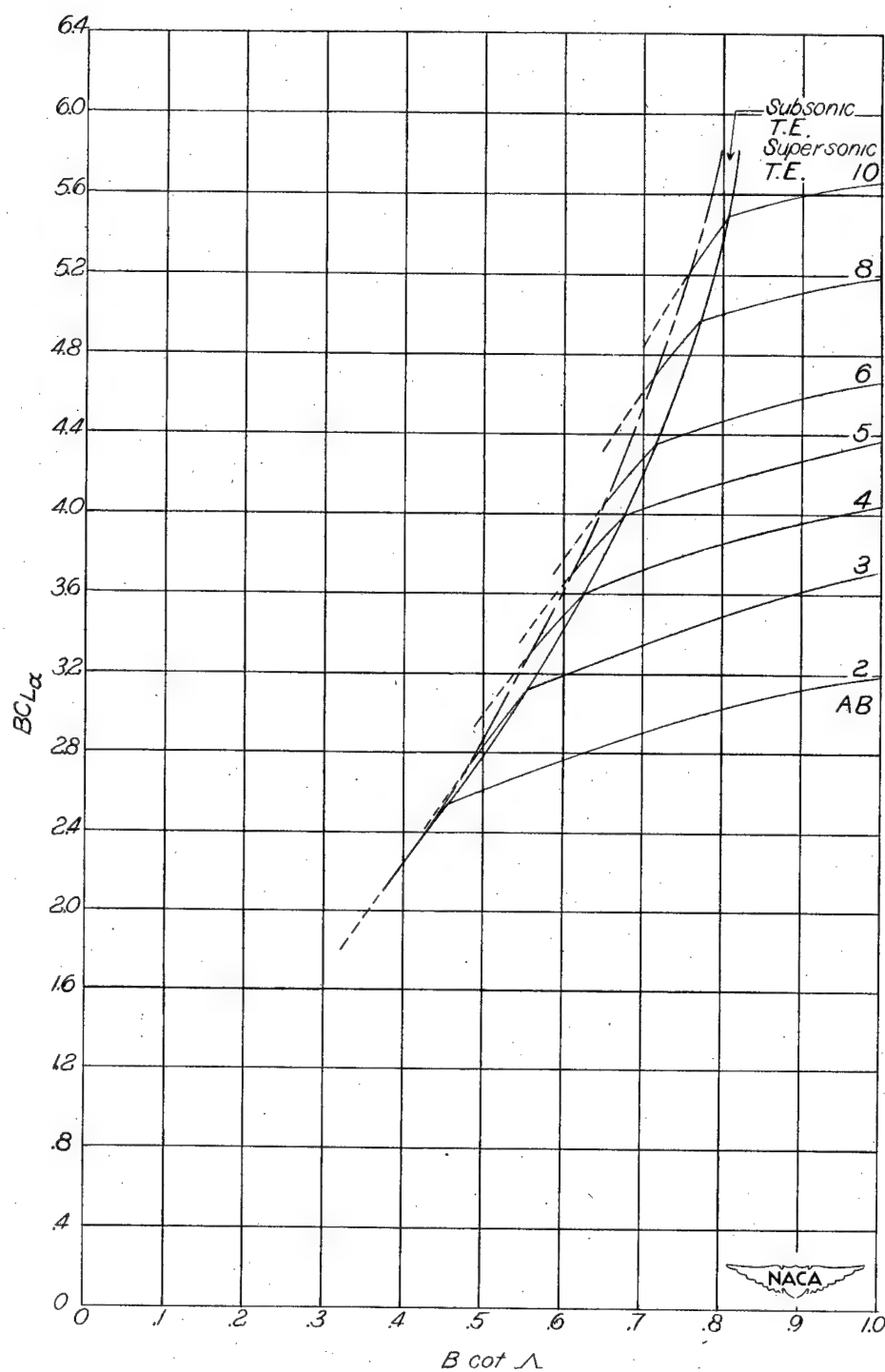
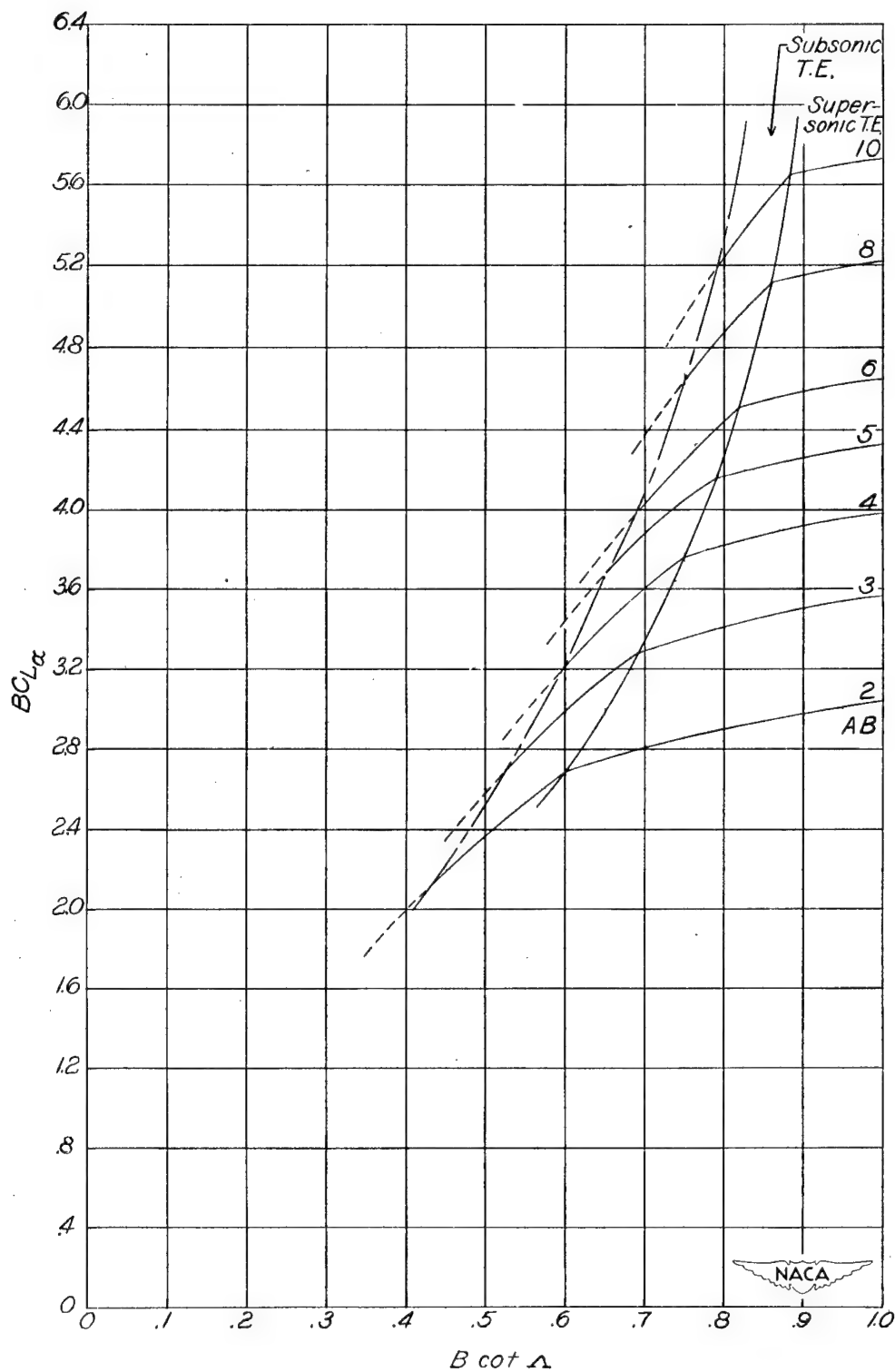
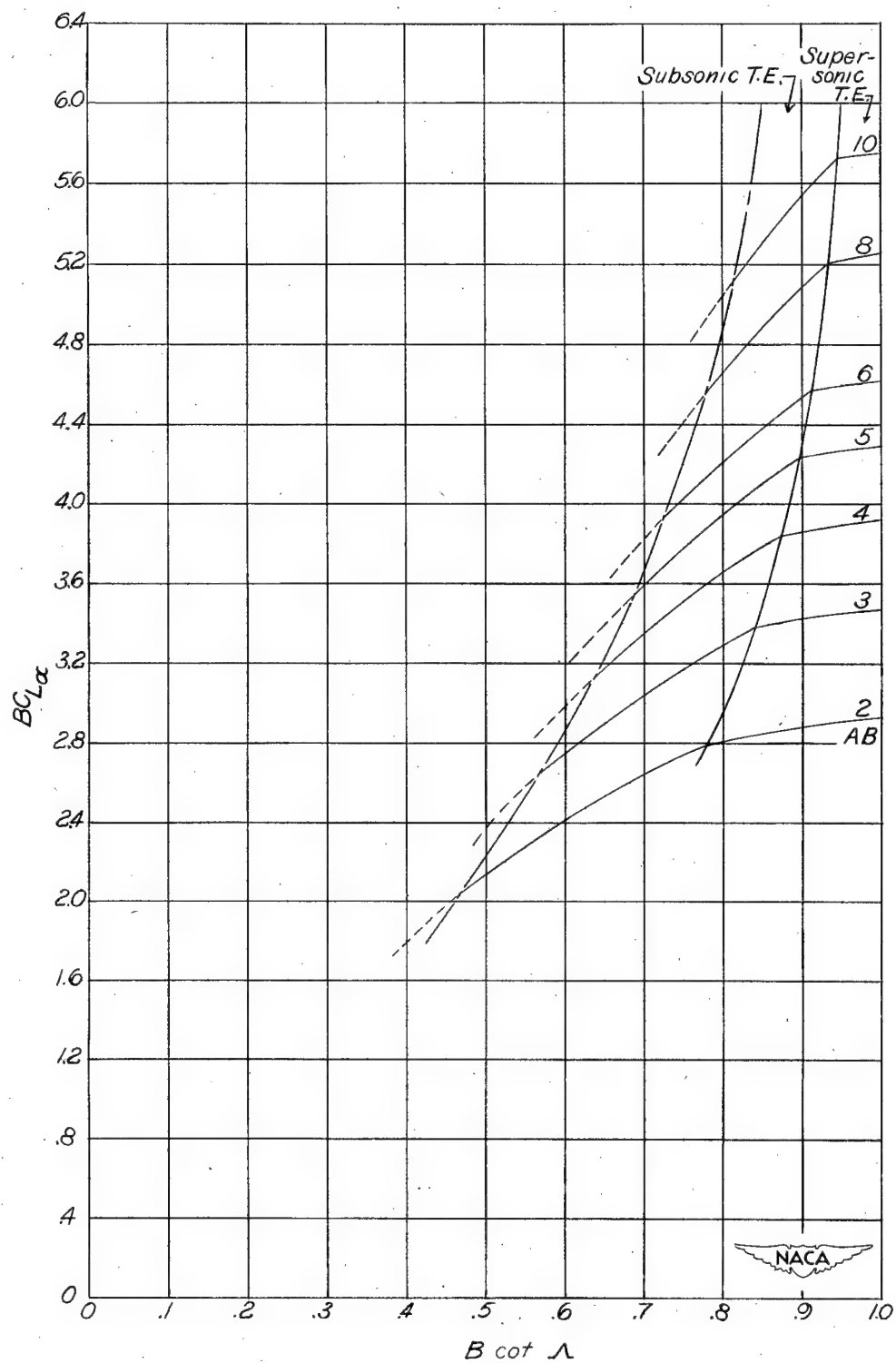
(a)  $\lambda = 0.25$ .

Figure 9.- Variation of  $BC_{L\alpha}$  with  $B \cot \Lambda$  for various values of  $BA$  and  $\lambda$ . Dashed parts of curves have limited significance. (See section entitled "Results and Discussion.")



(b)  $\lambda = 0.50$ .

Figure 9.- Continued.



(c)  $\lambda = 0.75$ .

Figure 9.- Concluded.

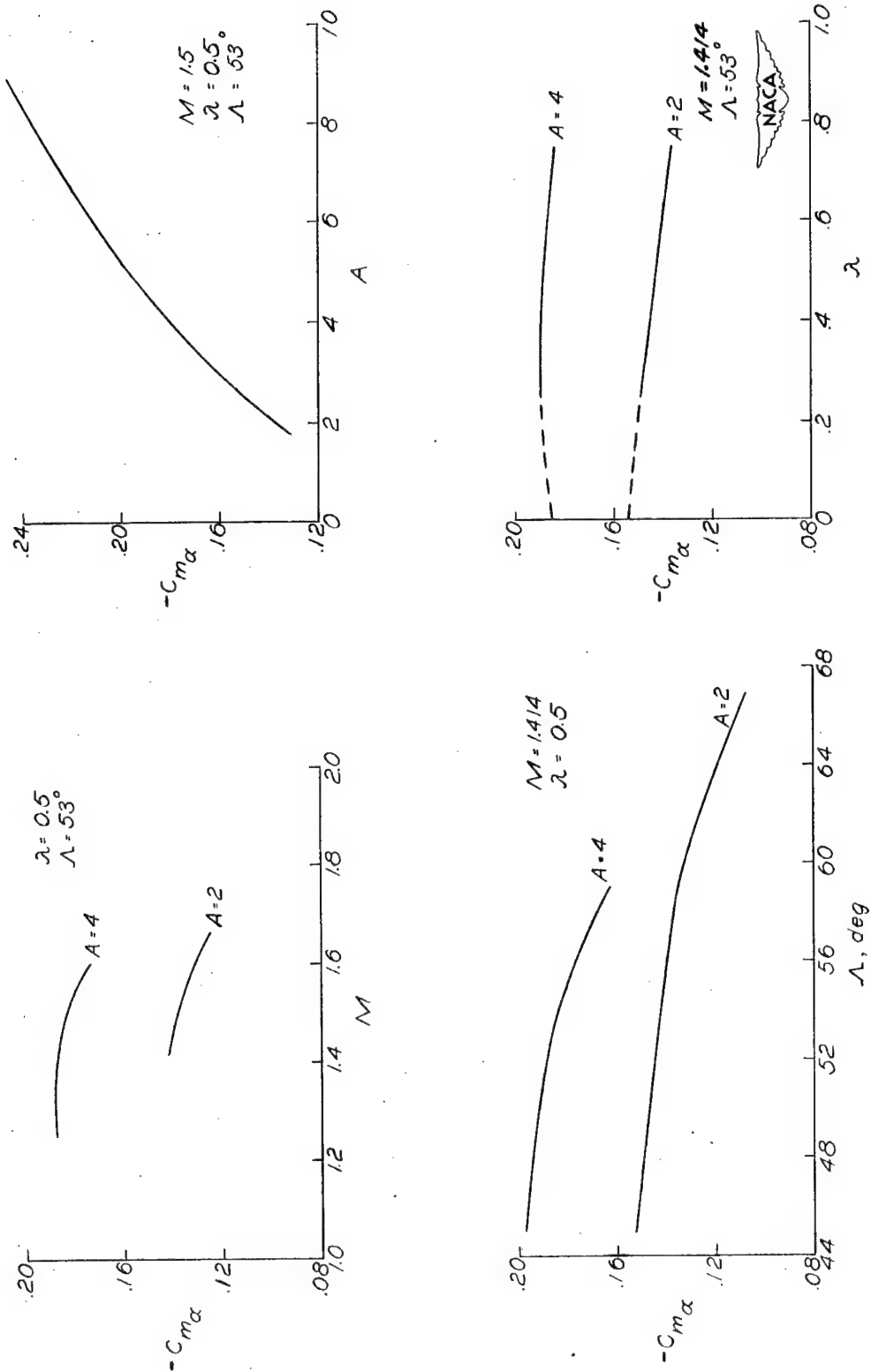


Figure 10.- Some illustrative variations of the static-pitching derivative  $C_{m\alpha}$  with Mach number, aspect ratio, sweepback, and taper ratio. Stability axes system; static margin, 0.05. Dashed parts of the curves for variations of  $C_{m\alpha}$  with  $\lambda$  represent an extrapolation from  $\lambda = 0$  to  $\lambda = 0.25$ .

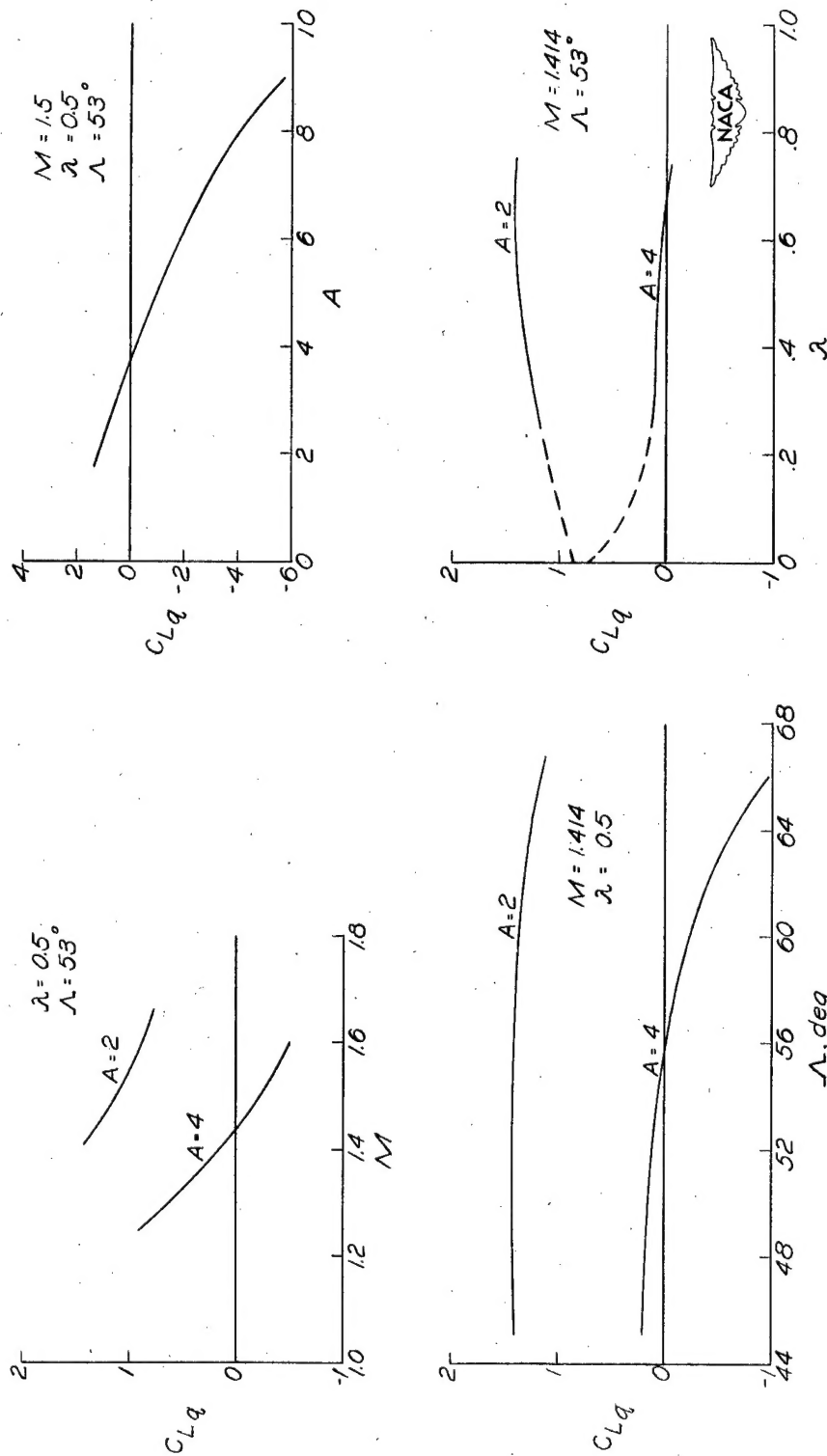


Figure 11.- Some illustrative variations of the lift-due-to-pitching derivative  $C_{Lq}$  with Mach number, aspect ratio, sweepback, and taper ratio. Stability axes system; static margin, 0.05.

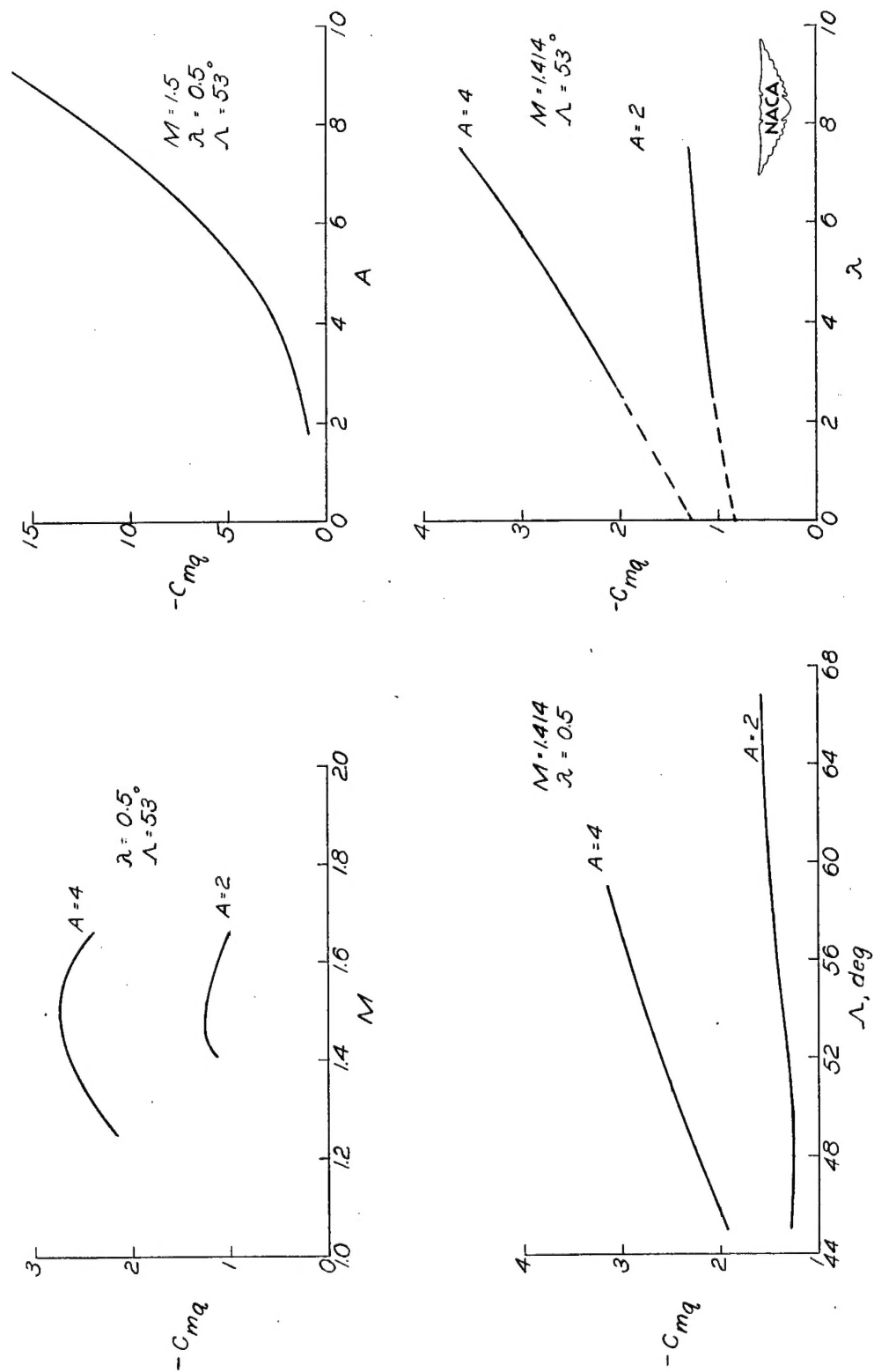






Figure 12.- Some illustrative variations of the damping-in-pitch derivative  $C_{mq}$  with Mach number, aspect ratio, sweepback, and taper. Stability axes system; static margin, 0.05.

<p>Wings, Complete - Theory</p> <p>1.2.2.1 S</p> <p></p> <p>Lift and Pitching Derivatives of Thin Sweptback Tapered Wings with Streamwise Tips and Subsonic Leading Edges at Supersonic Speeds.</p> <p>By Frank S. Malvestuto, Jr., and Dorothy M. Hoover</p> <p>NACA TN 2294 February 1951</p> <p>(Abstract on Reverse Side)</p>	<p>Wings, Complete - Aspect Ratio</p> <p>1.2.2.2.2 S</p> <p></p> <p>Lift and Pitching Derivatives of Thin Sweptback Tapered Wings with Streamwise Tips and Subsonic Leading Edges at Supersonic Speeds.</p> <p>By Frank S. Malvestuto, Jr., and Dorothy M. Hoover</p> <p>NACA TN 2294 February 1951</p> <p>(Abstract on Reverse Side)</p>
<p>Wings, Complete - Sweep</p> <p>1.2.2.2.3 S</p> <p></p> <p>Lift and Pitching Derivatives of Thin Sweptback Tapered Wings with Streamwise Tips and Subsonic Leading Edges at Supersonic Speeds.</p> <p>By Frank S. Malvestuto, Jr., and Dorothy M. Hoover</p> <p>NACA TN 2294 February 1951</p> <p>(Abstract on Reverse Side)</p>	<p>Wings, Complete - Taper</p> <p>1.2.2.2.4 S</p> <p></p> <p>Lift and Pitching Derivatives of Thin Sweptback Tapered Wings with Streamwise Tips and Subsonic Leading Edges at Supersonic Speeds.</p> <p>By Frank S. Malvestuto, Jr., and Dorothy M. Hoover</p> <p>NACA TN 2294 February 1951</p> <p>(Abstract on Reverse Side)</p>



### Abstract

Theoretical approximations to the static-pitching derivative  $C_{m\alpha}$ , the lift-due-to-pitching derivative  $CL_q$ , and the damping-in-pitch derivative  $C_{mq}$  were derived for a series of sweptback tapered wings. The lift-curve slope  $CL_\alpha$  has been included for completeness. The results are valid for a range of Mach number for which the leading edge is subsonic and the trailing edge, either supersonic or subsonic provided the trailing-edge Mach lines do not intersect the leading edge of the wing.

Design curves are presented which permit rapid estimations of the derivatives for given values of aspect ratio, taper ratio, Mach number, and leading-edge sweep.

### Abstract

Theoretical approximations to the static-pitching derivative  $C_{m\alpha}$ , the lift-due-to-pitching derivative  $CL_q$ , and the damping-in-pitch derivative  $C_{mq}$  were derived for a series of sweptback tapered wings. The lift-curve slope  $CL_\alpha$  has been included for completeness. The results are valid for a range of Mach number for which the leading edge is subsonic and the trailing edge, either supersonic or subsonic provided the trailing-edge Mach lines do not intersect the leading edge of the wing.

Design curves are presented which permit rapid estimations of the derivatives for given values of aspect ratio, taper ratio, Mach number, and leading-edge sweep.

### Abstract

Theoretical approximations to the static-pitching derivative  $C_{m\alpha}$ , the lift-due-to-pitching derivative  $CL_q$ , and the damping-in-pitch derivative  $C_{mq}$  were derived for a series of sweptback tapered wings. The lift-curve slope  $CL_\alpha$  has been included for completeness. The results are valid for a range of Mach number for which the leading edge is subsonic and the trailing edge, either supersonic or subsonic provided the trailing-edge Mach lines do not intersect the leading edge of the wing.

Design curves are presented which permit rapid estimations of the derivatives for given values of aspect ratio, taper ratio, Mach number, and leading-edge sweep.

### Abstract

Theoretical approximations to the static-pitching derivative  $C_{m\alpha}$ , the lift-due-to-pitching derivative  $CL_q$ , and the damping-in-pitch derivative  $C_{mq}$  were derived for a series of sweptback tapered wings. The lift-curve slope  $CL_\alpha$  has been included for completeness. The results are valid for a range of Mach number for which the leading edge is subsonic and the trailing edge, either supersonic or subsonic provided the trailing-edge Mach lines do not intersect the leading edge of the wing.

Design curves are presented which permit rapid estimations of the derivatives for given values of aspect ratio, taper ratio, Mach number, and leading-edge sweep.